

ACCEPTED MANUSCRIPT • OPEN ACCESS

Systematic assessment of the biocompatibility of materials for inkjet-printed ozone sensors for medical therapy

To cite this article before publication: Lisa Petani *et al* 2021 *Flex. Print. Electron.* in press <https://doi.org/10.1088/2058-8585/ac32ab>

Manuscript version: Accepted Manuscript

Accepted Manuscript is “the version of the article accepted for publication including all changes made as a result of the peer review process, and which may also include the addition to the article by IOP Publishing of a header, an article ID, a cover sheet and/or an ‘Accepted Manuscript’ watermark, but excluding any other editing, typesetting or other changes made by IOP Publishing and/or its licensors”

This Accepted Manuscript is © 2021 The Author(s). Published by IOP Publishing Ltd..

As the Version of Record of this article is going to be / has been published on a gold open access basis under a CC BY 3.0 licence, this Accepted Manuscript is available for reuse under a CC BY 3.0 licence immediately.

Everyone is permitted to use all or part of the original content in this article, provided that they adhere to all the terms of the licence <https://creativecommons.org/licenses/by/3.0>

Although reasonable endeavours have been taken to obtain all necessary permissions from third parties to include their copyrighted content within this article, their full citation and copyright line may not be present in this Accepted Manuscript version. Before using any content from this article, please refer to the Version of Record on IOPscience once published for full citation and copyright details, as permissions may be required. All third party content is fully copyright protected and is not published on a gold open access basis under a CC BY licence, unless that is specifically stated in the figure caption in the Version of Record.

View the [article online](#) for updates and enhancements.

Review Article

Systematic assessment of the biocompatibility of materials for inkjet-printed ozone sensors for medical therapy

Lisa Petani, Valerie Wehrheim, Liane Koker, Markus Reischl, Martin Ungerer, Ulrich Gengenbach, and Christian Pylatiuk

Institute for Automation and Applied Informatics (IAI), Karlsruhe Institute of Technology (KIT), 76344 Karlsruhe, Germany

E-mail: petani@kit.edu

October 2021

Abstract. The biocompatibility of medical sensors is of great importance. In order to prevent harm of the patient during measurement, this aspect must be considered throughout the entire design process. Biocompatibility can be achieved by various methods. For example, the sensor can be encapsulated, only biocompatible materials can be used for the sensor, or anti-inflammatory agents can be applied to the surface of the sensor. In this paper the focus is on sensors fully fabricated from biocompatible materials. Two exemplary inkjet-printed amperometric and impedimetric sensors are systematically assessed regarding their biocompatibility. Both sensors can be used for the measurement of dissolved ozone during oxygen-ozone injection therapy. For the sensors each material is evaluated with respect to the international standard ISO 10993. Overall, many amperometric and impedimetric sensors are fabricated from a small set of materials. The assessment reveals that for this specific application an amperometric sensor consisting of gold and silver nanoparticle inks, inkjet-printed on a polydimethylsiloxane membrane, and passivated with SU-8 ink offers the highest biocompatibility and reaches a good compliance with other important requirements. In addition, biological characterization tests are required for the specific medical application to validate the biocompatibility. From this study, it can be concluded that the findings on biocompatibility can also be transferred to other sensors that are made of the same set of materials but are for other applications. This applies to oxygen, glucose, pH, hydrogen peroxide, sweat lactate, and acetone sensors.

Keywords: Inkjet-printing, biocompatibility, nanoparticle ink, ozone sensors, amperometric measurement, impedimetric measurement, medical applications

Submitted to: *Flexible and Printed Electronics*

1. Introduction

Various amperometric and impedimetric sensors, such as ozone, glucose, sweat lactate, and acetone sensors, utilize the same or an overlapping material set for their fabrication. These sensors are conventionally manufactured with metal evaporation, chemical gold plating [1], or screen printing [2]. In general, organic and printed electronic (OPE) technologies can be used to fabricate such sensors in additive process steps. An alternative to conventional manufacturing is inkjet-printing (IJP). It offers the broad flexibility of a digital manufacturing process. Layouts can be easily adapted and IJP is an emerging and leading technology for low-waste and low-cost production [3]. In case the sensor is inkjet-printed, the measuring element as well as substrate, passivation, membrane and, if applicable, light or heating element can be manufactured by means of controlled dispensing of small droplets of the particular ink followed by post-processing steps. If applied in the medical field, all these sensors have in common that the investigation of the biocompatibility has a very high priority because the sensors are in direct contact with human body liquids and tissues. Biocompatible means that the body does not exhibit a negative response to the sensor, such as allergic or toxic. The sensor has to be produced under sterile conditions or sterilized after the production to be free of infectious germs [4].

Previous work investigated applications of ozone sensors for different medical applications and the current approaches of inkjet-printed ozone sensors and developed an experimental setup for novel ozone sensors [5, 6]. In order to further expand this research, we examined the biocompatibility of the materials, utilized for two exemplary amperometric and impedimetric ozone sensor approaches. Thereby, the findings can be transferred to the other sensors mentioned above.

1.1. Requirements for medical sensors

Depending on the specific application, medical sensors need to meet requirements, such as sensitivity, selectivity, short response and recovery time, long-term stability, aqueous or gaseous measurement environment, measuring at room temperature (RT), and the requirement or absence of a light activation element. Here, amperometric, impedimetric metal oxide semiconductors (MOS), impedimetric carbon nanotube (CNT), absorption, and photoluminescence sensors are focused. In previous work [5], the measurement principles and specific requirements for the ozone measurement during the oxygen-ozone therapy are explained in more detail. The measurement principles and their corresponding properties are listed in Table 1 [7]. For medical applications, where it is currently not possible to measure the in-vivo concentration, an average sensitivity is mostly sufficient. Very small changes of the concentration, e.g. in the tip of the needle of an injection syringe during oxygen-ozone therapy, do not lead to severe health problems. The selectivity of sensors can be increased with a semi-permeable membrane. Furthermore, a membrane enables the application of a gas sensor in aqueous environment. The membrane has to be permeable to the analyte and less or preferably

Biocompatibility for inkjet-printed ozone sensors

3

Table 1: Qualitative summary of the most important properties of dissolved ozone sensors [7].

Properties	Amperometric	Impedimetric (MOS)	Impedimetric (CNT)	Absorption	Photoluminescence
sensitivity	high	high	high	high	high
selectivity	poor	poor	medium	high	high
response time	medium	short	long	very short	long
recovery time	short	long	long	short	long
long-term stability	low	high	high	high	high
environment	aqueous	gaseous	gaseous	aqueous	aqueous
temperature	RT	high	RT	RT	RT
light activation	no	yes	no	yes	yes

not permeable to interfering substances [8]. For most of the investigated medical applications the long-term stability is a secondary property because many devices, such as the injection syringe, are single-use products. A low measurement temperature and the avoidance of an ultra violet (UV) light source as light activation element for the sensing material are crucial for sensors with body liquid and tissue contact because high temperatures (higher than body core temperature) and UV light can damage biomolecules.

In the following, the oxygen-ozone injection and the biocompatibility of materials used in inkjet-printed amperometric and impedimetric ozone sensors are considered. In addition, the transferability is considered in more detail.

1.2. Oxygen-ozone injection for the treatment of a disk herniation

In industrialized countries, both, the live expectancy and the daily sitting time have grown during the last century [9]. This involves the risk of physical health problems, such as strokes, heart diseases, diabetes mellitus, cancer, and back pain [10, 11]. Back pain, which is a major health problem, can be caused by muscle strain, arthritis, or disk herniation [12]. In case of a herniated disk the nucleus pulposus of a spinal disk is pushed out of the annulus fibrosus and may cause pressure on the spinal nerve [13]. The comparison of a herniated disk and a normal disk is shown in Figure 1. Disk herniation can be healed by surgery, physiotherapy, heat treatment, or oxygen-ozone therapy [14, 15]. Surgery always bears risks and physiotherapy and heat treatment only work for mild forms of disk herniation. Therefore, the oxygen-ozone therapy is a promising minimally invasive therapy. The oxygen-ozone mixture is injected into the disk [16] or surrounding tissue [15]. Ozone leads to the reduction of the water amount in the disk and thereby shrinks the volume. Thus, the pressure on the pinched nerve is reduced and the pain of the patient is relieved. Additional benefits of ozone therapy are that the immune system is enhanced and oxidative stress is reduced. Oxidative stress

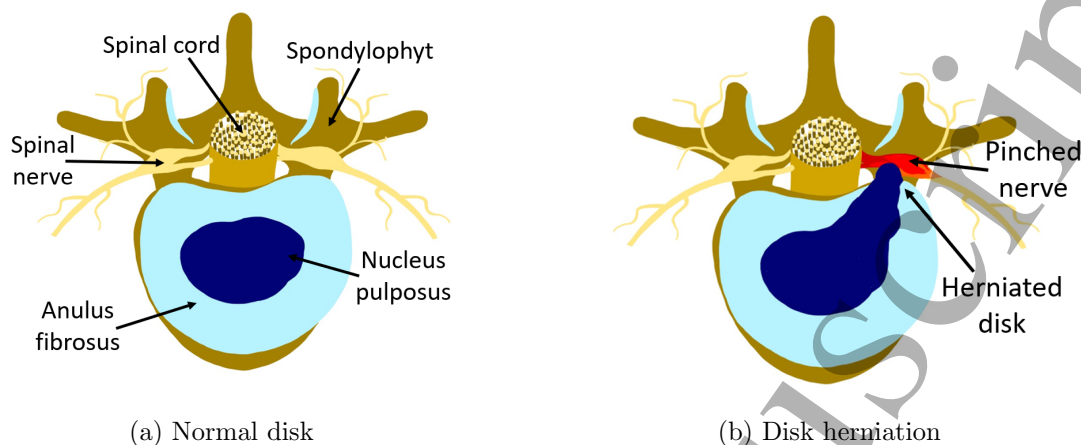
Biocompatibility for inkjet-printed ozone sensors

Figure 1: Comparison of a normal and herniated disk. In case of a disk herniation the inner part of the disk, the nucleus pulposus, causes pressure on the nerve.

indicates a disproportion between producing, accumulating, and detoxifying reactive oxygen species [17]. The ozone concentration has to be monitored in-vivo because ozone decays quickly and the amount of ozone after production in the injection syringe differs from the amount during the treatment. It is highly important to ensure that the applied concentration does not harm the patient but still treats the disk herniation effectively. For the measurement of the dissolved ozone concentration, the following measurement principles are suitable: amperometric, impedimetric with MOS or CNTs, absorption based, and photoluminescence. With regard to the concentration, a measurement has to be possible for dissolved ozone concentrations up to $70 \mu\text{g ml}^{-1}$ [6]. According to Table 1 most of the sensors can be operated at RT.

2. Materials and methods

In this paper, an application is focused in which ozone can be measured using two measuring methods. The respective sensors for these two measurement methods can be produced using IJP. Subsequently, a literature research is carried out, which is used to provide findings on the biocompatibility of the selected exemplary sensors. These statements are transferable to other sensors, such as oxygen, glucose, pH, hydrogen peroxide, sweat lactate, and acetone sensors because the same set of materials is used.

2.1. Assessment of the biocompatibility for medical sensors

According to the European Commission of Health and Consumers for the European Union, the Health Risk Assessments of the Food and Drug Administration (FDA) for the United States of America, and the National Medical Product Administration for China, medical devices can be subdivided into three groups depending on their health risk. The groups reach from low risk devices (group I), such as bandages and wheelchairs

Biocompatibility for inkjet-printed ozone sensors

5

to devices with a high health risk (group III), such as hip prostheses, heart catheters, and pacemakers [18]. Ozone sensors for oxygen-ozone injection are in between these two groups (group IIb according to the European Commission of Health and Consumers), which includes the contact with body fluids for a short duration.

There are different approaches to achieve biocompatibility, such as encapsulation of the sensor, utilization of only biocompatible materials, and application of anti-inflammatory agents to the surface of the medical device. For the encapsulation, membranes (porous or non-porous) can be employed, whereby hydrogels are most widely utilized for the application in medical devices [19]. The application of anti-inflammatory agents to the surface of the medical device reduces the inflammation in the body, whereby nonsteroidal anti-inflammatory drugs (NSAIDs), like acetylsalicylic acid (e.g. aspirin), or glucocorticoids, such as dexamethasone, can be injected into the encapsulation [20,21]. Figure 2 shows the properties for functionality and biocompatibility, which have to be assessed for the sensor and production process according to ISO 10993 [22].

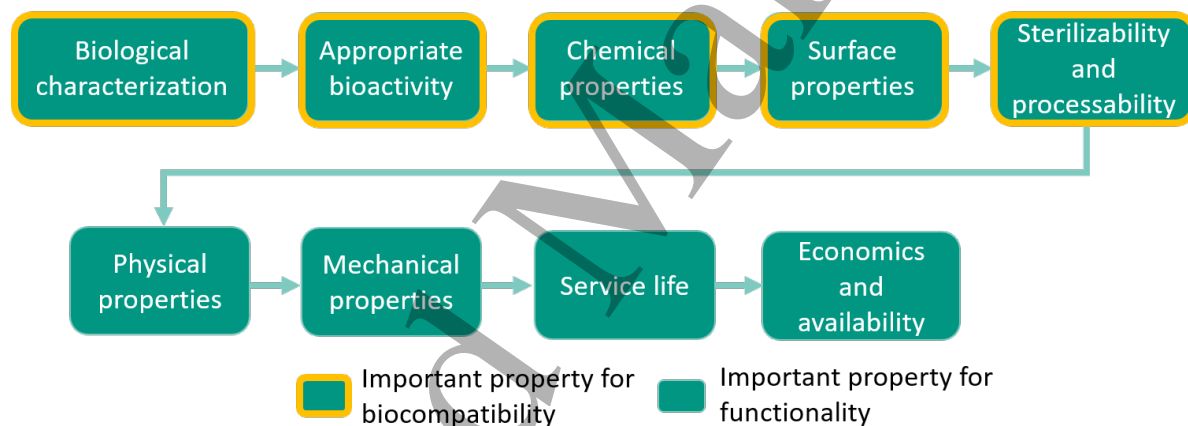


Figure 2: Properties of materials according to the international standard ISO 10993 [22], whereby the properties are ordered in descending order of importance for the biocompatibility. The main factors for biocompatibility are marked by a yellow frame. Criteria that are displayed without a yellow frame have only minor impact on biocompatibility.

In the following, the important properties for biocompatibility are explained. For biological characterization, the behaviour of the material in a living biological environment is investigated [23]. Therefore, biological characterization tests have to be conducted, whereby the tests depend on the type of contact with the body tissue and the contact time. For our application, the single-use sensor has contact with the intervertebral disk tissue for a short amount of time and has no contact with blood of the circulatory system [16]. This leads according to ISO 10993 [22] to the group assignment 2A and from this the required tests are derived. If there was additional contact of the sensor with blood of the circulatory system, an additional test of hemocompatibility would be required. According to ISO 10993 [22], the subsequent tests are necessary

Biocompatibility for inkjet-printed ozone sensors

to ensure the biocompatibility of the final sensor for our application: Cytotoxicity, sensitization, irritation and intracutaneous reactivity, pyrogenicity, and acute systemic toxicity. Cytotoxicity tests are used to investigate the influence of the material on surrounding cells [22]. They can be performed in-vitro and represent the first step to investigate the biocompatibility of a material. Sensitization tests are applied to determine the risk of allergic reactions [22]. These tests have to be conducted in-vivo. Irritation and intracutaneous reactivity tests are necessary to evaluate the local reaction of tissue [24]. For this test, the application route and the contact duration are needed [22]. In-vitro tests are only available to test pure chemicals and not the final sensor. The irritation and intracutaneous reactivity of a medical device is tested in-vivo for the final sensors [22]. Pyrogenicity tests evaluate if materials lead to inflammatory reactions in the body [22]. Therefore, in-vitro and in-vivo tests for the materials are necessary. Furthermore, the acute systemic toxicity has to be investigated. Systemic toxicity tests examine the distribution of a toxic substance from its point of entry to various parts of the body where it can damage cells. The systemic toxicity of materials can only be studied using in-vivo tests because this requires a living organism to represent the system. All tests must be performed for all materials used.

The appropriate bioactivity investigates the response of the material to the host and can be classified into toxic, biotolerable, bioinert, bioactive, and degradable [23,25]. For our application the sensor has to be non-toxic and bioinert. In addition, the sensor is a disposable product and should therefore be biodegradable or at least recyclable due to the impact on the environment.

Characterization of chemical properties can complement biological testing and is important for determining biocompatibility. In addition, the characterization of the chemical properties can be applied to identify differences between established and newly evolved devices, which can reduce the amount of in-vivo tests further [26]. For the characterization, each manufacturing substance, the material composition and physical structure, and the interactions between the material and body liquids or tissues need to be determined.

Furthermore, the surface properties need to be investigated for the determination of the biocompatibility because surface modifications (surface oxidation or coating) influence the interactions between material and biological system and thus the biocompatibility [25, 27]. This includes the characterization of the surface tension, wettability, and surface roughness of a material [23].

In addition, the sterilizability and processability are essential for a medical device. The sterilization process can alter the biocompatibility because the material's surface and characteristic may be modified [28]. Preferably, the sensor is manufactured under sterile conditions, thereby minimizing any pathogenic contact.

Biocompatibility for inkjet-printed ozone sensors

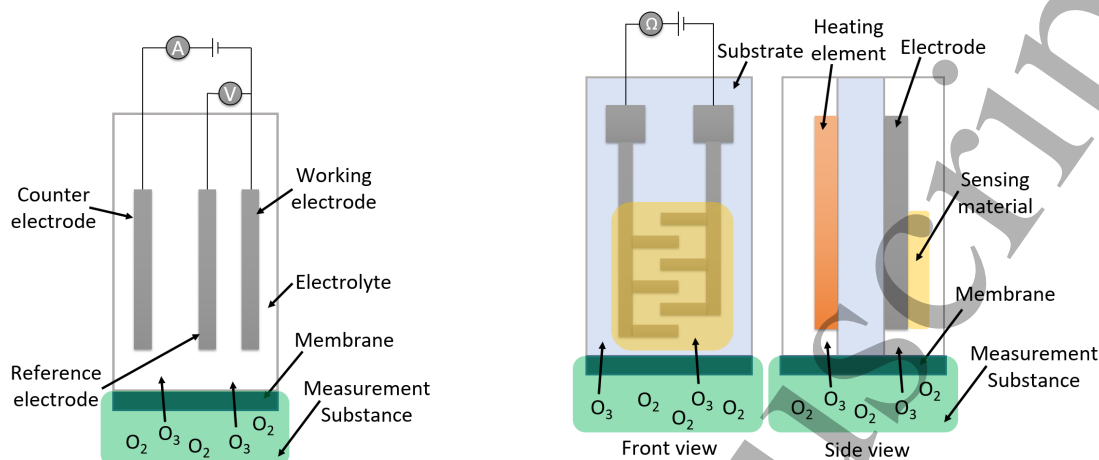
7

2.2. Amperometric and impedimetric sensors for ozone measurement

Summarising Section 1.1 and Table 1, for the application requirements of a dissolved ozone sensor during oxygen-ozone therapy, amperometric and impedimetric sensors are further investigated. Amperometric sensors are most promising because of the best fulfilment of the requirements and the simplicity of the design. The main advantages of amperometric sensors compared to the other measuring principles are the absence of a heating or light activation element and the possibility to realize the measuring principle in a very small assembly space. Impedimetric sensors based on MOS are also further assessed because of the shorter response time. In order to achieve short response times, MOS usually require a heating or light activation element, which may affect the health of the patient. Although a light activation or heating element is normally required, impedimetric sensors are considered here further due to their low response time and very small space requirements. Optical ozone sensors that are manufactured with current technology yield very good measurement results. The major challenge of miniaturizing optical sensors is that they require relatively large optical path lengths in the centimetre range. This is one of the reasons why a miniaturized optical ozone sensor is not yet available. In addition, optical absorption sensors also need UV light for ozone measurement, which is critical in combination with body liquids and tissues. Photoluminescence and impedimetric CNT sensors have too high response times for our application.

Therefore, sensors that are built up by layer systems, in particular by printable layer systems, are considered in this paper, such as amperometric and impedimetric sensors. The schematic illustrations of the amperometric and impedimetric sensor principles are shown in Figure 3 and are explained in detail in previous work [5]. An amperometric sensor consists of three electrodes, working electrode (WE), counter electrode (CE), and reference electrode (RE), and detects changes in electric current caused by a chemical reaction [29]. The applied constant voltage between WE and RE needs to be high enough to ensure a complete reaction of the ozone at the WE but lower than the voltage that leads to decomposition of the electrodes. The electrolyte solution is between the electrodes and the membrane and the reduction reaction of ozone at the WE results in a current flow that can be measured [30]. Impedimetric sensors measure the concentration by determining changes of the conductivity. They consist of a sensing material, electrodes, and a substrate. In addition, a heating or light activation element improves the sensor's response time.

Biocompatibility for inkjet-printed ozone sensors



(a) Three-electrode amperometric sensor, whereby changes of the current due to a chemical reaction are measured at the WE.

(b) Impedimetric sensor, changes of the conductivity of the sensing material are determined in order to obtain the concentration.

Figure 3: Schematic of an amperometric and impedimetric sensor.

Examples of commercially available impedimetric and amperometric ozone sensors are shown in Figure 4. These commercial sensors cannot be used for ozone measurement during oxygen-ozone injection for the treatment of a herniated disk because they have too large dimensions, insufficient long-term stability and too high cross-sensitivity to other chemical substances. For this reason, it is important that ozone sensors are further developed.

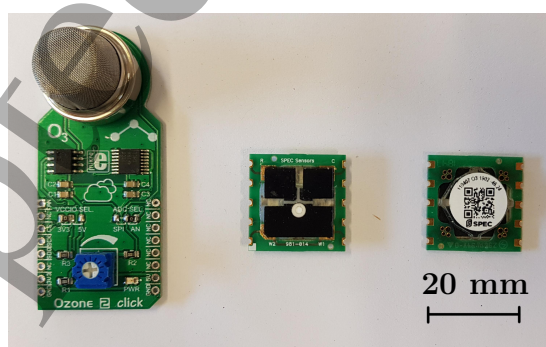


Figure 4: Commercial impedimetric ozone sensor MIKROE-2767 (MikroElektronika, Belgrade, Serbia) on the left and commercial amperometric ozone sensors SDK-O3 (SPEC Sensors, California, USA) on the middle and right.

2.3. Structure and materials of ozone sensors

For amperometric dissolved ozone sensors, appropriate materials are necessary for the electrodes, substrate, membrane, passivation, and electrolyte. Mostly, the electrodes

Biocompatibility for inkjet-printed ozone sensors

9

consist of precious metals, such as gold (Au), silver (Ag), and platinum (Pt), or are combined with non-metal materials, such as silver chloride (AgCl) for the RE or boron-doped diamond (BDD) for the WE [31–35]. For the substrate aluminium (Al), alumina (Al_2O_3) [36, 37], glass [38–40], quartz [41, 42], silicon dioxide (SiO_2)/silicon (Si) [43], fused silica [44], Si [45], or borosilicate wafers [44] can be applied. Polymers, such as polyimide (PI) [46], polyethylene terephthalate (PET) [31], poly(methylmethacrylate) (PMMA) [47], polytetrafluoroethylene (PTFE) [48], polyvinyl alcohol (PVA) [49], polyvinyl chloride (PVC) [31], and polydimethylsiloxane (PDMS) [50–52] can also be utilized as substrate. Here, the specific application requires a flexible substrate, which enables the integration of the sensor on the needle of an injection syringe. For amperometric sensors, a membrane is necessary to ensure selective measurement. Therefore, a material that acts as both substrate and membrane is preferred. The membrane needs to be non-porous to reduce the permeation of oxidizing substances that interfere with the measurement, such as oxygen. For the membrane various materials, such as Al_2O_3 [36,37], zirconium dioxide (ZrO_2) [36], PDMS [53], PTFE [36,48,54], and polyvinylidene difluoride (PVDF) [54], can be applied. For this particular application, PDMS is superior because it has four times the gas permeability for ozone than for oxygen [53] and can be processed with IJP [50]. For the passivation SU-8 is a commonly applied passivation ink [48, 55]. In addition, potassium nitrate (KNO_3), potassium sulfate (K_2SO_4), and sodium chloride (NaCl) are frequently utilized as an electrolyte for amperometric sensors.

Impedimetric sensors consist of two electrodes, a sensing material, a substrate, a membrane, and a heating or light activation element. The electrodes are based on noble metals [56, 57], copper (Cu) [58], titanium (Ti) [59], and tin-doped indium oxide (ITO) [42]. As sensing material zinc oxide (ZnO) [43], tungsten trioxide (WO_3) [60], indium oxide (In_2O_3) [61], stannic oxide (SnO_2) [62], and CNTs [63–65] can be employed. Materials for the substrate and membrane can be chosen analogous to amperometric sensor materials. The material of the heating element needs good thermal conductivity and the same materials can be utilized as for the electrodes. For the light activation element indium gallium nitride (InGaN)/gallium nitride (GaN) [66], InGaN [67], or aluminium gallium nitride (AlGaIn) [68] can be applied. For the light source and light activation elements of impedimetric sensors, the same materials can be used as for optical ozone sensors. The latter commonly consist of a light source and a photodetector with a sensing material. The photodetector with sensing material is based on a glass or quartz substrate, which is covered by a sensing material. The sensing material can be made of ZnO [69], methylene blue [70], or poly(3,4-ethylenedioxythiophene) (PEDOT) doped with polystyrene-sulfonate (PSS) forming PEDOT:PSS [71, 72].

Table 2 shows an overview of currently utilized materials for the main components of amperometric, impedimetric, and optical sensors, as well as substrates and membranes. For the application of a sensor during oxygen-ozone therapy, the amperometric measurement principle followed by the impedimetric measurement principle is most promising.

Biocompatibility for inkjet-printed ozone sensors

10

Table 2: Overview of currently utilized materials for the main components of dissolved ozone sensors, consisting of sensing material, electrodes, light activation or heating element, substrate, and membrane.

Amperometric	Impedimetric	Optical	Substrates	Membranes
Au, Ag [31,32]	Au [56,57]	ZnO [69]	Al [40]	Al ₂ O ₃ [36,37]
Pt [31,32]	Ag [56,57]	PEDOT:	Al ₂ O ₃ [36,37]	ZrO ₂ [36]
Ag/AgCl [33]	Pt [56,57]	PSS [71,72]	glass [38–40]	PDMS [50,52]
BDD [34,35]	Cu [58]		quartz [41,42]	PTFE [48]
	Ti [59]		SiO ₂ /Si [43]	PVDF [54]
	ITO [42]		Si [45], PI [46]	
	ZnO [43]		PET [31]	
	WO ₃ [60]		PMMA [47]	
	In ₂ O ₃ [61]		PTFE [48]	
	SnO ₂ [62]		PVA [49]	
	InGaN [67]		PVC [31]	
	CNT [63–65]		PDMS [50,52]	

Table 3 provides a toxicity rating for single oral doses tested for rats according to Mumford et al. [73] using the values for the lethal dose (LD).

Table 3: Toxicity rating for single oral doses tested for rats. Modified according to [73].

Rating	Description	LD ₅₀ [mg kg ⁻¹]
1	extremely toxic	≤ 1
2	highly toxic	1-50
3	moderately toxic	50-500
4	slightly toxic	500-5000
5	practically non-toxic	5000-15000
6	relatively harmless	>15000

Furthermore, Table 4 shows an overview of the material toxicity for the materials of Table 2. The quantity of a consumed chemical that kills 50% of a sample set is defined as LD_{50} . There are different methods (oral, inhalation, or skin contact (dermal)) to determine toxicity in different animals (mice, rats, or rabbits). For the table, oral was focused for rats, as these were the only values available for almost all materials. Nanoparticle (NP) toxicity is also affected by the NP size, shape, surface charge, and alterations [74].

Table 4: Overview of material toxicity for the materials of Table 2.

Material	LD ₅₀ [mg kg ⁻¹] ^a	Conditions	Toxicity Rating	Ref.
Ag	280	rats, oral	3	[76]
	800	rabbits, oral	4	
AgCl	> 5000	rats, oral	5	[77]
Al	1000	oral	4	[78]
Al ₂ O ₃	> 2000	rats, oral	4	[79]
Au	> 2000	rats, single dose, 10-50 nm NPs	4	[80]
BDD	NR	NR	NR	
CNT	> 5000	single-wall CNT	5	[81]
Cu	LD ₁₀₀ = 30 mg kg ⁻¹	rats, copper sulphate	-	[82]
	LD = 10-20 g	humans, copper sulphate	-	[83]
glass	NR	NR	NR	
InGaN	NR	NR	NR	
In ₂ O ₃	396	mice, oral	3	[84]
ITO	> 10000	rats, oral	5	[85]
PDMS	> 4800	rats, oral	4	[86]
PEDOT	650	oral	4	[87]
PSS	> 8000	rats, oral	5	[88]
PET	> 8000	rats, oral	5	[89]
PI	NR	NR	NR	
PMMA	> 8400 - 9400	rats, oral	5	[90]
Pt	> 5000	rats, oral	5	[91]
PTFE	> 11280	rats, oral	5	[92]
PVA	5000	rats, oral	5	[93]
PVC	> 10000	rats, oral	5	[94]
PVDF	6000	rats, oral	5	[95]
quartz	> 2000	rats, oral	4	[96]
Si	3160	rats, oral	4	[97]
SiO ₂	10000	rats, oral	5	[98]
SnO ₂	> 20000	rats, oral	6	[99]
TiO ₂	> 5000	no systemic toxicity, mice and rabbits, oral, 129.4 nm NP	5	[100]
WO ₃	> 5000	rats, oral	5	[101]
ZnO	> 5000	single dose, oral	5	[102]
ZrO ₂	> 5000	rats, oral	5	[103]

NR: not reported; ^a unless otherwise stated; Ref.: Reference

2.4. Inkjet-printing as manufacturing method

For ozone sensors the following conventional fabrication methods are mostly applied: spin-coating, dip-coating, screen-printing, UV photolithography, and spray-coating [5]. Compared to the fabrication methods stated above, IJP is a digital printing technique, whereby compared to screen-printing or UV photolithography neither masks nor templates are needed, which decreases set-up time and costs. Another advantage of IJP compared to spin-coating, dip-coating, and spray-coating is the easy adaptability of the printing patterns and the possibility of printing on flexible substrates. Moreover, by mounting the print head or substrate respectively on a four-axis handling system, IJP has the potential to print ozone sensors directly onto syringe needles used in ozone therapy for herniated disks. One additional advantage compared to the above-mentioned processes is that IJP is a non-contact process. This means less mechanical stress on the substrate and fewer sources of contamination, such as mask residue. Inkjet-printing methods are distinguished into two methods: continuous IJP and drop-on-demand IJP [75]. Whereas in continuous IJP, droplets are delivered continuously at a preset frequency, in drop-on-demand IJP, the actuation electronics dispense a droplet only at the desired target position [75]. Thus, drop-on-demand IJP, which is considered in this paper, allows individual adjustment of the drop size as well as the number of drops sent per trigger to control the total amount of material delivered to the target [75]. Nevertheless, initial costs for the ink and printer are expensive [104]. Inks contain NPs as functional elements and solvents for printability. The solvent is subsequently removed by drying and curing and the NPs agglomerate on the substrate surface. Compared to photolithography and gravure printing, the resolution of IJP is only average at 10 μm to 50 μm . Furthermore, it is possible to change the drop size by the waveforms during IJP [105]. When higher resolutions of 1 μm are needed, specialized inkjet-printers, such as electrohydrodynamic inkjet-printers or micro-plotters, are necessary [106–109]. For the IJP process, the utilized inks and substrates have to be compatible and need to be adjusted. A parameter that needs to be adjusted between the substrate and ink is the sintering temperature. High sintering temperatures to form a coherent porous NP layer, which may be required for selected inks, can exceed the substrate's glass transition or melting temperature and thereby impair the substrate's functionality, stability, and biocompatibility. For economic manufacturing of these sensors, piezoelectric drop-on-demand IJP, as shown in Figure 5, is a promising opportunity because for this additive manufacturing process no mask or template is needed and the process can be controlled digitally. Furthermore, printing on flexible substrates is possible and the ink can be applied contactless and at low temperatures [110,111]. Sterilization processes can also be integrated into manufacturing process chains based on IJP. In general, sterilization of the sensor can be realized by heat, ionized radiation, disinfection with aqueous solutions, or the low-temperature-gas-method [112]. Ideally, the medical device is produced directly under sterile conditions [112]. This can minimize any pathogenic contact [112].

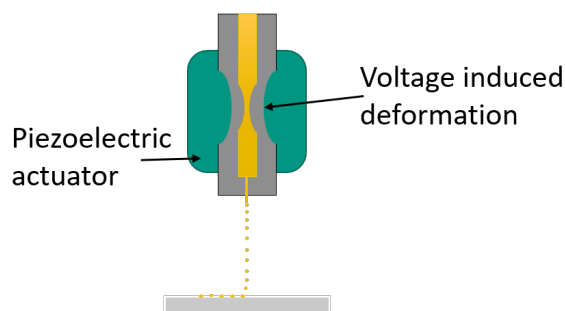


Figure 5: Nozzle for drop-on-demand IJP, whereby ink is applied with a piezoelectric actuator on a substrate and the actuator does not get into contact with the substrate.

Figure 6 shows the IJP system MIBBS2 [111]. A substrate, here a PET film, is currently on the vacuum-chuck in the middle of the image, whereby the substrate can be printed. The axes can be moved with the game controller. There is also an emergency stop next to the game controller. Hidden behind is the actual piezo controller with which the waveform can be set.

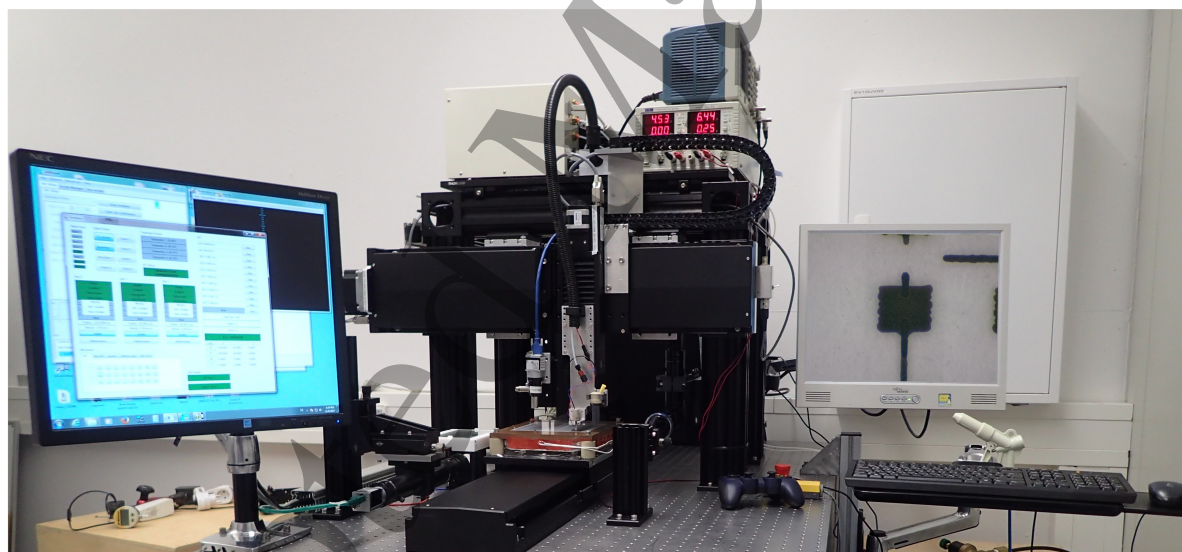


Figure 6: Inkjet-printing system MIBBS2 reported by Gengenbach et al. [111]. The left screen shows the user interface of the printer where the parameters are set and the right screen shows the detail view of the inspection camera. In the centre of the image is the vacuum chuck on which a substrate is printed. Above it is the print head and the printer reservoir. At the top left is the controller for the vacuum pressure of the printing head.

2.5. Assessment of an exemplary amperometric and impedimetric sensor

The materials in Table 5 are investigated in the following in terms of their individual biocompatibility. They are applied for amperometric and impedimetric ozone sensors.

Table 5: Component materials of assessed amperometric and impedimetric dissolved ozone sensors.

Component	Amperometric Sensor	Impedimetric Sensor
electrodes	Au and Ag NP inks	Pt
sensing material	NA	In ₂ O ₃
substrate	PDMS	Al ₂ O ₃
membrane	PDMS	PDMS
passivation	SU-8	NA
electrolyte	KNO ₃ , K ₂ SO ₄ , and NaCl	NA
heating element	NA	Pt
light activation	NA	InGaN

NA: not applicable.

Amperometric sensor The investigated sensor is based on a previously published oxygen sensor [113] and can be manufactured with IJP. The sensor reported by previous research [113] and the sensor which is here examined are both amperometric sensors, which react in general to all oxidizing substances. Selective measurement for ozone can be enabled by a suitable membrane. A PTFE membrane can be utilized for an oxygen sensor [113] and a PDMS membrane for an ozone sensor. For the WE and CE a gold nanoparticle (AuNP) ink (Au-LT-20 by Fraunhofer IKTS, Germany) is chosen, for the RE a silver nanoparticle (AgNP) ink (DGP 40LT-15C by ANP, Korea) is evaluated, and for the passivation of the electrodes a SU-8 ink (XP PriElex SU-8 1.0 by MicroChem, USA) is selected. For the membrane and substrate PDMS (Sylgard 184 Elastomer Kit by Dow Corning, USA) is applied. The most important properties for processing the inks with an inkjet-printer are shown in Table 6. Solvents, solid fraction, and NPs sizes influence the properties of the printed layers such as homogeneity, conductivity, porosity, and coffee ring effect [114]. Depending on the viscosity different printing heads have to be chosen or solvents have to be added. Furthermore, the viscosity and surface tension have an effect on the drop formation and thereby on the IJP process [114]. The curing temperature is especially important for the selection of the substrate. In addition, the post-processing can lead to cracks or coffee ring effects and thereby has an influence on the conductivity of the final printed structure [114]. For the electrolyte KNO₃, K₂SO₄, and NaCl are investigated.

Impedimetric sensor Here, an exemplary impedimetric dissolved ozone sensor is assessed, which can be manufactured with IJP and is based on a conventionally manufactured ozone sensor by Takada et al. [115]. As well as the conventionally manufactured sensor, the IJP sensor consists of an Al₂O₃ substrate, an In₂O₃ sensing material, and Pt for the electrodes and the heating element. The sensor, which is assessed in the following sections, consists in addition of a PDMS membrane. Furthermore, InGaN is studied as light activation element, which can be employed

Table 6: Overview of material properties of Au and Ag NP inks, SU-8 ink, and PDMS ink used for an exemplary amperometric sensor.

Properties	Au-LT-20 (Au)	DGP 40- LT-15C (Ag)	XP PriElex SU-8 1.0 (SU-8)	Sylgard 184 PDMS (PDMS)
solid fraction [wt.-%]	19.6	30 - 35	32	NA
NP size [nm]	30	50	NA	NA
viscosity [mPa·s]	7.3	10 - 17	9.68	10 - 20
surface tension [mN m ⁻¹]	35.1	35 - 38	30	20 - 35
curing temperature [°C]	150 - 200	120 - 150	135	25 - 200
post-processing	thermal	thermal	UV & thermal	thermal

NA: not applicable.

alternatively to the heating element. Here, a platinum nanoparticle (PtNP) ink (PT-LT-20 by Fraunhofer IKTS, Germany) is investigated, which is water-based and has a solid fraction of 20 wt.-%, a NP size of max. 200 nm, a sintering temperature of 200 °C, a surface tension of 38 mNm, and a viscosity of 12 mPa·s.

2.6. Approach for the biocompatibility assessment

First, literature references to bulk materials, inkjet-printed sensors, and the respective inks are evaluated. Then, the influence of the manufacturing process on the biocompatibility of the materials is considered. Finally, references on the transferability of the assessments are evaluated.

3. Results

3.1. Biocompatibility of nanoparticle inks

Inks containing metallic NPs are commonly employed, for example, for the electrodes or heating element. The NPs are sintered, connect with the substrate surface, and form a coherent porous layer. There are two risk factors for the biocompatibility assessment. Firstly, non-connected NPs can remain on the printed structure if not all NPs are sintered during the production process and thus detach. Secondly, in case of a flexible sensor, it is possible for NPs to detach when the sensor is used. In particular, NPs that are not completely or well bound can detach. The sintering process only works when the solvent and the coating of the NPs are removed. If there is still a substantial amount of residue, the layer does not sinter completely and the highest possible conductivity is not reached. However, in some cases post-processing i.e. solvent expulsion, stabilizer removal, and the actual sintering is done in a single oven process step. It is not certain

Biocompatibility for inkjet-printed ozone sensors 16

that all the solvent is removed. Stabilizers and other organic components are even more difficult to remove. Furthermore, the insertion of the sensor into the spinal disk is an additional risk, as shear forces occur. For this reason, in techniques based on NPs, the NPs must be considered separately in terms of risk. The majority of the NPs must be bound, otherwise there is no conductive layer. It can be ensured by conductivity measurements of the printed structure that the layer has not completely dissolved into individual NPs. In terms of measurement, the target conductivity can be used for quality control to test whether there are cracks in the layer. This means that several printed structures are first produced, which are subjected to inspection with a microscope. The conductivity of these printed structures is then determined, which corresponds to the target conductivity. For further tests, the value for the target conductivity can be used to perform a quality control with a single measurement. However, minimal amounts of NPs can still detach, which does not affect the conductivity but has an influence on the biocompatibility. For this reason, consideration and subsequent testing are necessary. The biocompatibility of NP inks depends on the NP's size, shape, surface chemistry, and surface charge [116]. An increased particle size leads to a higher surface reactivity, mass diffusivity, sedimentation velocity, and attachment efficiency, while a decreased particle size results in a higher surface-to-volume ratio and thus a higher risk of cytotoxicity [117]. Furthermore, the particle size has an influence on the system toxicity, although it is still unknown whether larger or smaller particles are more toxic [118,119]. Moreover, the NP's agglomeration highly affects the biocompatibility of the ink [120]. For example larger titanium dioxide (TiO_2) aggregates have a higher effect on the cell viability than smaller ones [121]. In addition, a different shape of the NPs may alter the penetration into a cell, such as spherical NPs are less toxic and reactive than fibre-shaped NPs [120,122,123]. A larger contact area leads to a lower penetration efficiency into a cell but also bears a higher risk of cytotoxicity [124,125]. Additionally, the cytotoxicity is also affected by the molecular structure and bonding types at the surface of the NPs because these properties change the recognition of the NPs at biomolecules, such as cells or proteins [126]. If particles are recognized as foreign to the body, an immunological reaction can occur. Furthermore, the surface charge, depending on the density and polarity, may affect the biocompatibility. Overall, a higher surface charge density results in a higher toxicity, in contrast to neutral or slightly charged surface charge densities [127]. For example, positively charged NPs have a more toxic effect on non-phagocytic cells [128–130] and negatively charged NPs have a negative effect on phagocytic cells [120]. Overall, size, morphological features, surface structure, and surface charge can have a significant influence on the biocompatibility of a medical device. There are also additional influences on the biocompatibility, depending on the specific material, which are assessed in the following for the exemplary sensors.

3.2. Exemplary amperometric sensor

In the following, an exemplary amperometric sensor is assessed for its biocompatibility. Previous research has already examined the cytotoxicity of the Au, Ag, and SU-8 ink by culturing hepatocytes onto a membrane, which was on top of printed patterns [48]. The authors reported a maintained viability of the cells, which indicates the non-cytotoxicity of these materials for the given setup [48]. The biocompatibility of the processed ink is crucial here. Thus, the properties of NPs that already adhere to a surface must be considered. Figure 7 shows a computer-aided design (CAD) version of an amperometric sensor according to 3a, whereby this design is currently being realised using IJP technology and will subsequently be published separately.

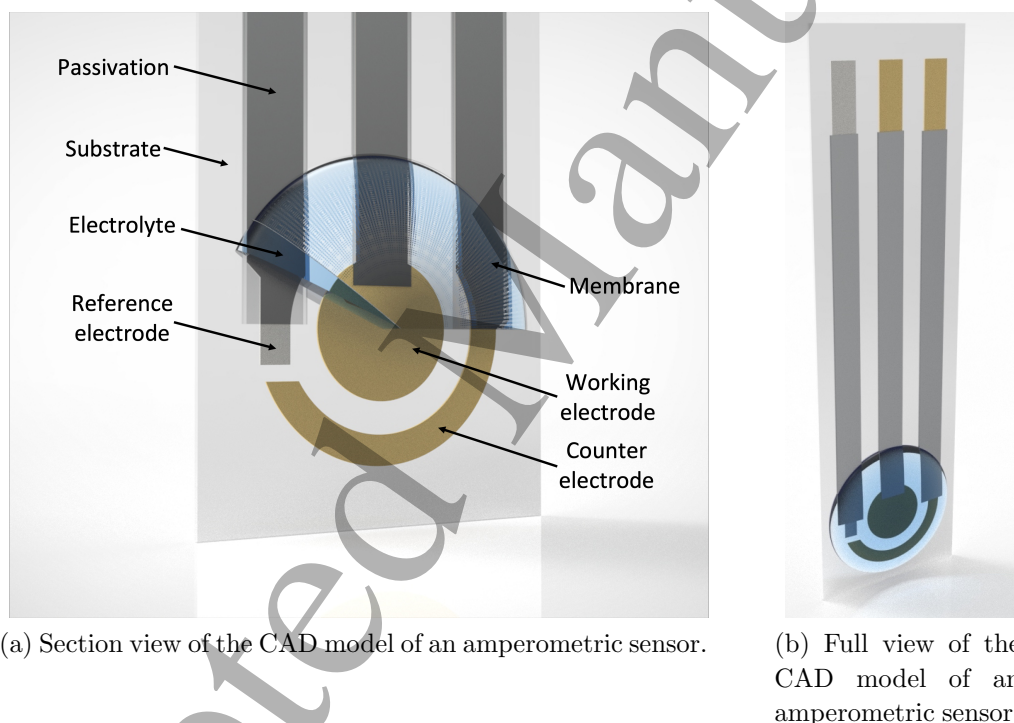


Figure 7: CAD drawing of an amperometric sensor, including counter electrode, working electrode, reference electrode, electrolyte, membrane, substrate, and passivation.

3.2.1. Gold nanoparticle ink as working and counter electrode material AuNPs are applied for biomedical applications, such as medical imaging, drug delivery systems, and cancer treatment because of their optical properties and potential biocompatibility, depending on the NP shape, NP size, surface chemistry, and surface charge [116]. For the exemplary amperometric sensor, the Au ink according to Table 5 is analyzed in terms of the ink's biological and printing properties. Thereby, the AuNP ink is applied for the WE and CE of the amperometric sensor, which is depicted in Figure 7. The NPs are dissolved in water and ethylene glycol and according to the manufacturer the

Biocompatibility for inkjet-printed ozone sensors 18

material is non-toxic and biocompatible. Hepatocytes cultured on a membrane on top of the printed ink show non-toxicity as the cells retain viability [48]. Furthermore, the solvent ethylene glycol has to be considered, as it is toxic for humans [131]. Ethylene glycol has a boiling point of 196 °C [132] and some residues may remain after curing or sintering below this temperature.

3.2.2. Silver nanoparticle ink as reference electrode material AgNPs are employed in medicine, such as in wound dressing and catheters [133], due to their antimicrobial properties [18, 134]. Here, AgNP ink is employed for the RE of the amperometric sensor, shown in Figure 7. A higher concentration, as applied for a medical ozone sensor, may have toxic effects on human cells [134]. The nucleus pulposus of a herniated disk can be approximated as aqueous environment. In an aqueous environment AgNPs release Ag ions that can bind to sulphur groups in biomolecules [134]. This can result in cytotoxicity, genotoxicity, or immunological responses. In addition, AgNPs have the ability to pass through the blood brain barrier, thus they are classified as neurotoxin [135]. The morphology of AgNPs in various inks differs and affects the biological properties. For the exemplary amperometric sensor, the Ag ink according to Table 6 is analyzed in terms of the ink's biological and printing properties. The AgNPs are solved in triethylene glycol monoethyl ether (TGME) and the ink has a good adhesion to polymer and glass substrates. The encapsulation of the AgNPs is made of polyvinylpyrrolidone (PVP) [136]. Lee et al. [136] state that at the specified curing temperature the PVP becomes liquid and remains in the structure or on the substrate, i.e. is not completely expelled. The ink is not classified as a hazardous substance according to the regulation (EG) No. 1272/2008 [137] and does not include carcinogenic components in concentrations of more than 0.1% [137, 138]. Previous research reported a good biocompatibility of this ink using cultured hepatocytes onto a membrane on top of the printed material [48]. The solvent TGME does not contain any components classified as toxic [139]. The boiling temperature of 256 °C for TGME is higher than the curing temperature of the ink, thus residuals of TGME remain in the final sensor. Before drying, the printed ink may be rinsed with polar solvents, such as ethyl alcohol or isopropyl alcohol (IPA), and treated with a vacuum treatment for the complete evaporation of the solvent. For great amounts of ethyl alcohol, taken in orally or through the blood stream, occurs hepatotoxicity, which can cause liver injuries [140]. The rinsing of the printed structure is supposed to be non-hazardous as ethyl alcohol and IPA are main disinfectants in the medical sector. However, the utilized amount has to be minimized to ensure the biocompatibility of the product.

3.2.3. Polydimethylsiloxane as substrate and membrane material Polydimethylsiloxane is used for the substrate and membrane illustrated in Figure 7. Thereby, the substrate consists of highly cross-linked PDMS and the membrane of PDMS with controlled permeation properties. This enables membrane properties that are necessary for the respective application, for example high permeability for ozone and low permeability for

oxygen for an amperometric ozone sensor. Due to the PDMS substrate, it is necessary that the curing of the gold and silver ink is done with photonic sintering. Photonic sintering is less destructive to the substrate as it does not heat up. For the amperometric sensor, a membrane is necessary to ensure selective ozone measurement. Non-porous PDMS is assessed as promising membrane material for the specific application. The functionality of the membrane depends for example on the porosity and the type and amount of functional groups on the surface. Polydimethylsiloxane is characterized as hydrophobic, non-flammable, non-toxic, and bioinert [141]. It is employed in medicine, such as for contact lenses or as a shell of breast implants [142]. Furthermore, PDMS is printable, for example Sylgard 184 ink can be applied to print an elastomer matrix [50, 51]. The viscosity of Sylgard 184 is 3500 mPa·s and has to be reduced prior to the printing process by additional solvents, such as octyl acetate (OA) [50, 51]. Afterwards, the ink has the viscosity and surface tension as stated in Table 6 [50]. Mikkonen et al. [50] and Sturgess et al. [51] did not detect residues of OA after printing and curing of the PDMS layer. The biocompatibility of PDMS is reported, however, the authors also stated a dependence of the biocompatibility on the production and post-processing methods [143]. For an ensured biocompatibility of PDMS, a full polymerization of the PDMS's oligomers and the removal of all short-chained molecules need to be ensured. Lee et al. [144] also reported the in-vitro biocompatibility of a PDMS (Sylgard 184) coated device.

3.2.4. SU-8 ink as passivation material For the passivation of the electrodes, which is displayed in Figure 7, SU-8 is utilized. Parts of the electrodes, which are not supposed to be exposed to the measurement substance, have to be passivated to avoid short-circuits. Furthermore, in case of a porous substrate, the pores need to be sealed with a passivation material [48]. There are various types of SU-8 available, such as SU-8 2002 and XP PriElex SU-8 1.0. SU-8 2002 was primarily developed for the spin coating process but can also be applied for IJP, whilst XP PriElex SU-8 1.0 is an ink that was specifically developed for IJP. Previous research investigated SU-8 2002, whereby the solvent is cyclopentanone [48]. This ink was already tested with regard to its biocompatibility [48]. The jettable ink XP PriElex SU-8 1.0 is an epoxy-based photoresist that consists of resin, solvent, and a photosensitive component containing antimony. After curing, the printed layers form stable isolation and dielectric layers, which are also applied as passivation layers for sensors [55]. The cross-linked polymer network, which is induced by UV light and heat, provides a high chemical resistance, thermal stability (up to 315 °C) [145], and high mechanical strength. However, publications diverge on the subject of the biocompatibility of SU-8. Multiple biological characterization tests consistent with ISO 10993 [22] were conducted and most of them [145–147] agreed that SU-8 is non-toxic and non-irritant. Nevertheless, some studies show a certain degree of cytotoxicity for SU-8 [148]. The toxicity of antimony depends on its valency [145]. The detachable amount of antimony may be reduced by additional UV and heat exposure. There are several surface treatments, such as chemical treatment with acid and base, grafting

Biocompatibility for inkjet-printed ozone sensors 20

of the surface with polyethylene glycol, and oxygen plasma treatment, to improve the biocompatibility of SU-8 [48,145]. The oxygen plasma treatment leads to an increase in the oxygen and carboxyl groups on the surface and thus the wettability as well as the surface energy increases [48]. When processing SU-8, it is important that the solvents can be removed as much as possible after the ink has been applied. Finally, in-vivo tests are necessary to confirm or reject the biocompatibility.

3.2.5. Potassium nitrate, potassium sulfate, and sodium chloride as electrolyte material

For an amperometric sensor, an electrolyte covering the electrodes is necessary to ensure proper conductivity between the electrodes and thus the sensor's functionality. The electrolyte may become obsolete if the sensor is applied to measure in body liquids and tissues, such as the nucleus pulposus, because they naturally contain ions, which may act as electrolyte. Hereafter, the electrolytes KNO_3 , K_2SO_4 , and NaCl , shown in Figure 7, are assessed with regard to their biocompatibility. Potassium and sodium occur naturally inside the human body. Potassium regulates the blood pressure, water balance, and acidity levels and controls enzyme reactions. Potassium and sodium are responsible for the transmission of signals, such as neurotransmission and muscle contraction in the body [149,150]. Nitrates, taken in by food, get inside the body transformed into nitrites, which prevents haemoglobin from transporting oxygen and thus can lead to an oxygen deficiency in the cells [151]. In addition, nitrate is transformed into nitric oxide, which positively influences the blood flow rates and metabolism [152]. Previous studies were very controversial about nitrate and a correlating cancer risk, but current research indicates that usual occurring amounts of nitrate do not increase the risk of tumors [153]. Sulfates are essential inside the human body and in medicine, such as for cell growth processes and before a colonoscopy [154,155]. However, sulfates can also lead to an irritation of the eye or skin [150]. Potassium nitrate is utilized in tooth paste and in the food industry to increase the product durability [156]. In the European Union K_2SO_4 is added as food additive E515 [157] and there are no maximum addition limits. Sodium chloride is a main mineral for humans and can be highly diluted injected intravenously as an isotonic saline solution [149].

The most promising electrolyte with regard to the biocompatibility is NaCl because it can be injected as isotonic saline solution without causing harm. Most critical in terms of biocompatibility is the electrolyte KNO_3 .

3.3. Exemplary impedimetric sensor

In the following an exemplary impedimetric sensor is assessed for its biocompatibility.

3.3.1. Platinum as electrode material For electrode materials, mostly noble metals with a high electrical conductivity are employed [5]. Here, Pt is assessed because it has a high biocompatibility, is inert to body liquids, and has a low corrosivity and good mechanical strength [158,159]. Therefore, Pt is often utilized for medical devices, such

as pacemakers, catheters, or stents [160]. Inks consisting of Pt are made of PtNPs or a Pt solution, such as chloroplatinic acid hydrate [161]. Platinum NPs are more promising with regard to the biocompatibility, because Pt solutions commonly include toxic substances. Schubert et al. [162] reported a nearly 100% cell viability and the formation of a highly biocompatible surface for the PT-LT-20 NP ink. They conducted in-vitro experiments with the NP ink with regard to their cytotoxicity according to ISO 10993 [163].

3.3.2. Indium oxide as sensing material Commonly, In_2O_3 , ZnO , SnO_2 , and WO_3 are applied as sensing material for MOS sensors [61]. Here, In_2O_3 is chosen because of the high sensitivity, low cross-sensitivity, and short response and recovery time [164]. As sensing material for an impedimetric sensor, In_2O_3 is employed in a crystalline water-insoluble form [165], which works optimally at temperatures between 200 °C and 400 °C [164]. Inks made of In_2O_3 can not be obtained commercially but they can be produced from oxide precursors based on sol-gel [166] or NPs [167]. Compared to NPs, oxide precursors based on sol-gel need higher temperature treatments. Previous research by Hassan et al. [110] performed a lactate dehydrogenase (LDH) cytotoxicity assay for a combination of a printed sodium alginate insulator layer on top of a printed In_2O_3 layer. The assay yields a non-cytotoxic result. The applied In_2O_3 NP ink consists of deionized water and sodium polyacrylate. The diameter of the NPs is between 20 nm to 70 nm and the NP ink has to be thermally treated after the IJP process at 150 °C. The biocompatibility of In_2O_3 in combination with body liquids and tissues is not sufficiently investigated. Several studies investigated the inhalation of In_2O_3 , which yield toxic effects on the lungs [168,169]. Indium (III) ions injected into the blood stream are toxic to the kidney. In addition, hydrated In_2O_3 is by a factor of 40 more toxic than the corresponding ions [170]. Overall, there is not enough literature available to adequately determine the biocompatibility of In_2O_3 . Especially with regard to IJP In_2O_3 based inks, further research has to be conducted.

3.3.3. Alumina as substrate material As shown in Figure 3b, the electrodes and the heat or light activation element are separated by a substrate. The substrate needs to be compatible with the utilized ink for the electrodes and heating or light activation element and has to be heat conductive and heat stable. In the case of the exemplary sensor, Al_2O_3 is applied as substrate, which is a good heat conductor and insulator because of phonon resonance [171]. Alumina can be employed via IJP if Al_2O_3 NPs are dispersed into water or ethylene glycol [172]. Denes et al. [173] reported sufficient biocompatibility for Al_2O_3 based on the biological characterization tests provided by the international standard ISO 10993 [22]. In contrast, Mestres et al. [174] have identified that after an exposure to high concentration of small (20 nm) Al_2O_3 NPs, there is an increased release of reactive oxygen species (ROS) by macrophages. This results in oxidative stress, which may yield cell death. Moreover, additional chemicals required by the manufacturing method, such as solvents to make the material printable, may

Biocompatibility for inkjet-printed ozone sensors

22

further influence the sensor's biocompatibility.

3.3.4. Polydimethylsiloxane as membrane material The biocompatibility of PDMS has been already examined in Section 3.2.3 for the amperometric measurement principle.

3.3.5. Platinum as heating or indium gallium nitride as light activation element The biocompatibility of Pt has been already discussed in Section 3.3.1. For InGaN light emitting diodes (LEDs) in-vitro and in-vivo cytotoxicity tests, histology studies, and in-vivo immunological response analysis were conducted [175]. For the tested LEDs no cytotoxicity or immunological effects were reported [175]. In general, gallium nitrate can limit local inflammation due to its immunosuppressive effect [176,177]. The material of the LEDs shows a high biocompatibility. Instead, the use of UV light may be a bigger issue, because the exposure of UV light leads to a growth of the generation of ROS, which may damage biomolecules [178]. In addition, the UV light may damage directly or indirectly the deoxyribonucleic acid (DNA), depending on the UV light wavelength [179].

3.4. Potential alternatives with a higher biocompatibility

The utilization of biocompatible materials increases the probability of a finally biocompatible sensor, although the final sensor needs to be tested itself. Overall, the highest potential for biocompatibility of the materials in Section 2.5 show PDMS for the membrane and substrate and Pt and AuNP inks for the electrodes. In contrast, the lowest potential is present for AgNP inks for the reference electrode and In_2O_3 as sensing material. These materials may be substituted with Ti for the reference electrode and TiO_2 or ZnO as sensing material. Nevertheless, it is important to consider that the toxicity of TiO_2 and ZnO depends on the size and shape of the NP [180].

3.4.1. Titanium as reference electrode material and titanium dioxide as sensing material Titanium is often applied for medical applications, such as for prostheses and dental implants [25,28,181]. This is possible due to the good mechanical strength, excellent corrosion resistance, and extraordinary biocompatibility of Ti [182]. However, the main reason for the high biocompatibility is that the surface of Ti oxidizes to TiO_2 , which shows a non-toxic behaviour [182]. Despite the high biocompatibility compared to Ag, the electrical conductance of Ti is more than ten times smaller [183]. Nevertheless, it is possible to improve the electrical conductance by employing other noble metals, such as Pt, in combination with Ti [59]. Previous research has shown the applicability of TiO_2 as sensing material for impedimetric sensors [184] with a heating element for oxygen [185,186] and ozone [187] measurement. The resistance of TiO_2 is highly dependent on the temperature, therefore the wide application is limited by the high temperatures needed for the sensing material's functionality. Further research is necessary to increase the electrical conductance of Ti, decrease the needed

Biocompatibility for inkjet-printed ozone sensors

23

temperature for TiO₂ sensing material, and investigate the effects of the IJP process on the biocompatibility of the material.

3.4.2. Zinc oxide as sensing material In medicine ZnO is frequently applied, such as for drug delivery systems, bioimaging, and biosensors, for example glucose sensors [188]. Furthermore, it is a common sensing material for impedimetric sensors [59, 189]. Previous research reported the feasibility of gas measurement at RT with visible light enhancement [190, 191]. Further research is necessary to investigate the dissolved ozone measurement with these conditions. ZnO NP ink, whereby the NPs are dissolved in n-butanol, can be obtained commercially (Helios'Ink H-SZ01034 by GenesInk, France). The contact of n-butanol with eyes or skin leads to irritations [192]. In contrast, ZnO NPs have anti-inflammatory, anti-bacterial, and biodegradable properties. In addition, ZnO NPs are classified by the FDA as a safe substance [193].

3.5. Transfer of the assessment to other sensors

There are also several other sensors, such as hydrogen peroxide, glucose, pH, sweat lactate, oxygen, and acetone sensors, fabricated from the same material set (Au, Ag, PDMS, SU-8, KNO₃, K₂SO₄, NaCl, Pt, In₂O₃, Al₂O₃, and InGaN) as the previously described amperometric and impedimetric dissolved ozone sensors. The findings on the biocompatibility in this paper can be transferred to hydrogen peroxide sensors, e.g. reported by Wu et al. [1], which consist of a PDMS substrate, Au for the WE and CE, and Ag for the RE. Transfer is also possible for inkjet-printed electrochemical pH and glucose sensors, e.g. presented by Määtänen et al. [194]. Thereby, the WE and CE are made of Au, the RE consists of Ag, and PDMS is utilized for passivation [194]. For the pH sensor a polyaniline film is applied on the WE and for the glucose sensor a poly(3,4-ethylenedioxythiophene) layer is employed on the WE [194]. In addition, a transfer is possible for sweat lactate measurement with sensors that consists of an Ag electrode coated by Nafion with lactate oxidase as an enzyme [195]. There are also various similarities to a dissolved oxygen sensor made of AuNP ink for the WE and CE, AgNP ink for the RE, SU-8 ink for the passivation, and a polyethylene naphthalate (PEN) substrate [113]. An oxygen sensor, which operates at RT and is similar to the evaluated impedimetric sensor, can be also manufactured with Pt-doped In₂O₃ [196]. Furthermore, KNO₃, K₂SO₄, and NaCl are commonly applied electrolytes for amperometric sensors. Moreover, acetone sensors for biomedical applications, e.g. reported by Karmaoui et al. [2], contain Pt-decorated In₂O₃ NPs. Besides ozone measurement, In₂O₃ is often utilized for the IJP of transistors [110, 197, 198]. For medical applications, transistors can be applied for skin and health surveillance [199]. Additionally, InGaN-based chips are employed in laboratory medicine for refractometers to determine the total plasma protein in samples of blood and urine [200]. Overall, there are numerous applications in medicine that use the same set of materials as those employed for measuring dissolved ozone. For this reason, the assessments carried out here can be transferred easily.

4. Discussion

Biocompatible sensor materials increase the probability of an ultimately biocompatible sensor system. The use of non-toxic solvents and chemicals further increases the potential of an ultimately biocompatible sensor. However, the IJP process and post-processing steps can additionally influence the biocompatibility of the sensor by changing the material properties. Biocompatibility tests for the final sensor after all production steps have to be conducted. The biocompatibility of sensors in medical technology can be improved by a final heating step. This allows bound water to be removed, which can prevent corrosion of the electronics. It also removes volatile components of solvents. In the following, limitations of the current state of research and further research are discussed.

4.1. Limitations of the current state of research

The focus in this research lies upon amperometric and impedimetric sensors because these are currently most promising for an inkjet-printed sensor for the oxygen-ozone treatment of a disk herniation. Other materials for impedimetric sensors, such as a combination of MOS materials and CNTs or polymers, may be superior in the long-term after further research is conducted to improve the measurement with these materials. Polymers are commonly applied as sensing material for sensors but further research is necessary for application of polymers in ozone measurement [201]. Here, the sensor's miniaturization and stability are not considered. Especially the electrical potential of the RE has to be constant for different concentrations. In this research mostly the biocompatibility of the material in general instead of the specific IJP material is assessed, limited by the available literature. The IJP process and additional additives in the ink may affect the biocompatibility of the material. Various cytotoxicity tests were reported to indicate the cytotoxicity or non-cytotoxicity of a material. These tests have to be repeated for the cells present during the specific application, in this case in the intervertebral disk tissue, as the test results depend on both the cells and the material used. In addition, the biocompatibility of the sensor has to be in accordance with regulations, depending on the country in which the medical device is commercialized and manufactured. In the European Union the manufacturers have to comply to the Medical Device Regulation and in the United States of America to the FDA. Here, the international standard ISO 10993 [22] is considered because this is a standard for verifying that a product is biocompatible, which is very important for the technical documentation of a medical device.

4.2. Further research

Overall, the functionality and biocompatibility of an amperometric sensor for the oxygen-ozone therapy are most promising because of the measurement at RT, absence of UV light, and sufficient response time. It is still necessary to increase the

sensor's selectivity and a further decrease of the response time may be beneficial. Additional research is needed to test the final sensor produced via IJP through biological characterization tests. Nevertheless, in order to widely apply ozone sensors for various medical therapies, further measurement principles need to be investigated. The application of impedimetric and optical absorption sensors is mainly limited during medical therapy because of the high temperatures and UV light and may thereby be toxic for body liquids and tissues. Previous research [70, 202] has already reported the optical absorption ozone measurement in the visible spectral light range, but the requirement of long optical path lengths limits the application. Moreover, Wu et al. [203] also investigated the visible spectral light range. The authors reported the feasibility of light activation with blue light of Au/TiO₂-WO₃ as sensing material, but the response time above 200 s has to be improved. Further research is necessary to decrease the path length of optical absorption sensors or response time for the light activation with visible light for the application during medical therapies. In addition, a hybrid combination, reported by Wei et al. [204], of impedimetric MOS and CNT sensors is an opportunity to overcome the drawbacks of both sensor types, such as high measurement temperatures for MOS sensors and long response times for CNT sensors. Wei et al. [204] reported positive results at RT, but subsequent studies are necessary to further reduce the response time. Furthermore, the utilization of polymers needs to be further investigated. The main challenge for the measurement of the dissolved ozone during oxygen-ozone treatment is the approximation of body liquids inside the herniated disk as water. The interaction with body liquids and tissues may impair the functionality of the sensor. The body liquid may act as an electrolyte because of its ion concentration and therefore the additional sensor's electrolyte may become obsolete. Without an additional electrolyte, the manufacturing process of the sensor is simplified and the probability of the sensor's biocompatibility is increased because less substances are in contact with the human body.

5. Conclusion

Amperometric and impedimetric sensors are widely applied in medicine and often the same set of materials is utilized. Here, the application of a dissolved ozone sensor during the oxygen-ozone treatment of a disk herniation is focused. During this therapy and in general during therapies related to ozone it is crucial to monitor the ozone concentration [205]. The biocompatibility of sensors in medicine needs to be considered during the complete design and manufacturing process. In this research, an exemplary amperometric and impedimetric sensor are evaluated in compliance to the international standard ISO 10993 [22]. For the exemplary amperometric sensor, the following materials are selected: AuNP ink for the WE and CE, AgNP ink for the RE, SU-8 as passivation of the electrodes, PDMS as substrate and membrane, and KNO₃, K₂SO₄, or NaCl as electrolyte. The assessment of the exemplary amperometric sensor is the priority in this research because no heat or UV light activation is needed, which may negatively

affect body liquids and tissues. Thereby, the biocompatibility investigation already indicates a high potential for the exemplary amperometric sensor. For the exemplary impedimetric sensor, the following materials are chosen: Al_2O_3 for the substrate, Pt for the electrodes, In_2O_3 as sensing material, PDMS as membrane, and Pt for the heating element or InGaN as light activation element. The biocompatibility of the impedimetric sensor may be improved by using ZnO as sensing material, allowing measurements at RT with visible light. However, the feasibility of the measurement of ozone with these conditions still needs to be investigated. The materials for the exemplary sensors are also utilized for the measurement of oxygen, glucose, pH, hydrogen peroxide, sweat lactate, and acetone in medicine. Thus, the biocompatibility assessments can be transferred to these sensors. All of the investigated materials show potential for the application in a biocompatible sensor. Further examinations are important to test the biological and chemical characterization, bioactivity, cytotoxicity, sterilization, and packaging process for the sensors because these cannot be fully replaced by a literature review. In addition, research is necessary to investigate the possibility of eliminating the electrolyte by utilizing the ions inside the nucleus pulposus for the functionality of the sensor. The biodegradability and recycling process of the final sensor has to be considered to minimize the environmental impact of the single-use product. The potential of reaching a biocompatible device is increased by utilizing biocompatible or non-toxic materials. However, it still has to be considered that the properties and thereby the biocompatibility may be altered in the production process. For example, the surface properties are changed by combining several materials or by the sintering process. Through the sintering process, the porosity of printed NPs is decreased, which changes the electrical and surface properties. This may lead to a different reaction between the device and body liquids and tissues, which get into contact with the device. In addition, substances that are only necessary for the production process, may also affect the biocompatibility of the device. In order to get in contact with body liquids and tissues, the sensors need to be sterile, which can be reached by implementing a sterile IJP production process or by a final sterilization step. However, this reduction of the germ contamination may also affect the biocompatibility. Nevertheless, sterilization steps may not be necessary due to high sintering and curing temperatures, which may deactivate pathogens sufficiently. Overall, the biocompatibility depends on the applied materials, production method, surface properties, and contamination degree of the device with pathogens.

Acknowledgments

We thank Daniel Moser for creating the CAD model of the amperometric sensor. This research was supported by the Federal Ministry for Economic Affairs and Energy on the basis of a decision by the German Bundestag under Grant [ZF4717901SK9], the program Material Systems Engineering of the Helmholtz Association, and the program Natural, Artificial and Cognitive Information Processing (NACIP) of the Helmholtz-Association.

References

- [1] Wu W Y, Zhong X, Wang W, Miao Q and Zhu J J **2010** Flexible PDMS-based three-electrode sensor. *Electrochem. Commun.*, **12**, 1600–1604.
- [2] Karmaoui M, Leonardi S G, Latino M, Tobaldi D M, Donato N, Pullar R C, Seabra M P, Labrincha J A and Neri G **2016** Pt-decorated In₂O₃ nanoparticles and their ability as a highly sensitive (< 10 ppb) acetone sensor for biomedical applications. *Sens. Actuators, B*, **230**, 697–705.
- [3] Sui Y and Zorman C A **2020** Inkjet printing of metal structures for electrochemical sensor applications. *J. Electrochem. Soc.*, **167**, 037571.
- [4] Regulation (EU) 2017/745 of the European Parliament and of the Council of 5 April 2017 on medical devices, (accessed on 31 March 2021). Available online: <https://eur-lex.europa.eu/legal-content/EN/TXT/?uri=CELEX%3A32017R0745>.
- [5] Petani L, Koker L, Herrmann J, Hagenmeyer V, Gengenbach U and Pylatiuk C **2020** Recent developments in ozone sensor technology for medical applications. *Micromachines*, **11**, 624.
- [6] Petani L, Wüthrl L, Koker L, Reischl M, Renz J, Gengenbach U and Pylatiuk C **2021** Development of an experimental setup for real-time in-line dissolved ozone measurement for medical therapy. *Ozone: Sci. Eng.*, 1–11.
- [7] Korotcenkov G, Brinzari V and Ham M H **2018** Materials acceptable for gas sensor design: Advantages and limitations. *Key Eng. Mater.*, **780**, 80–89.
- [8] Reach G, Feijen J and Alcock S **1994** BIOMED concerted action chemical sensors for in vivo monitoring. The biocompatibility issue. *Biosens. Bioelectron.*, **9**, xxi–xxviii.
- [9] Owen N, Healy G N, Matthews C E and Dunstan D W **2010** Too much sitting: The population health science of sedentary behavior. *Exercise Sport Sci. Rev.*, **38**, 105–113.
- [10] Ihira H, Sawada N, Yamaji T, Goto A, Shimazu T, Kikuchi H, Inoue S, Inoue M, Iwasaki M and Tsugane S **2020** Occupational sitting time and subsequent risk of cancer: The Japan Public Health Center-based prospective study. *Cancer Sci.*, **111**, 974–984.
- [11] van Uffelen J G Z *et al.* **2010** Occupational sitting and health risks: A systematic review. *Am. J. Prev. Med.*, **39**, 379–388.
- [12] Estadt G M **2004** Chiropractic/Rehabilitative management of post-surgical disc herniation: A retrospective case report. *Journal of Chiropractic Medicine*, **3**, 108–115.
- [13] Raj P P **2008** Intervertebral disc: Anatomy - physiology - pathophysiology - treatment. *Pain Practice*, **8**, 18–44.
- [14] Airaksinen O *et al.* **2006** Chapter 4 European guidelines for the management of chronic nonspecific low back pain. *European Spine Journal*, **15**, 192–300.
- [15] Bocci V *Ozone. A new medical drug.*; Springer Netherlands: Dordrecht, Netherlands, 2011. ISBN: 978-90-481-9234-2.
- [16] Lehnert T, Naguib N N, Wutzler S, Nour-Eldin N E A, Bauer R W, Kerl J M, Vogl T J and Balzer J O **2012** Analysis of disk volume before and after CT-guided intradiscal and periganglionic ozone-oxygen injection for the treatment of lumbar disk herniation. *Journal of Vascular and Interventional Radiology*, **23**, 1430–1436.
- [17] Pizzino G, Irrera N, Cucinotta M, Pallio G, Mannino F, Arcoraci V, Squadrito F, Altavilla D and Bitto A **2017** Oxidative stress: Harms and benefits for human health. *Oxid. Med. Cell. Longevity*, **2017**, 1–13.
- [18] Chen Q and Thouas G A **2015** Metallic implant biomaterials. *Materials Science and Engineering: R: Reports*, **87**, 1–57.
- [19] Nafea E H, Marson A, Poole-Warren L A and Martens P J **2011** Immunoisolating semi-permeable membranes for cell encapsulation: Focus on hydrogels. *J. Controlled Release*, **154**, 110–122.
- [20] Onuki Y, Bhardwaj U, Papadimitrakopoulos F and Burgess D J **2008** A review of the biocompatibility of implantable devices: Current challenges to overcome foreign body response. *J. Diabetes Sci. Technol.*, **2**, 1003–1015.
- [21] Dinarello C A **2010** Anti-inflammatory agents: Present and future. *Cell*, **140**, 935–950.

- [22] Int. Standard ISO 10993-1. Biological evaluation of medical devices - Part 1: Evaluation and testing within a risk management process., October 2009.
- [23] Dahman Y *Biomaterials science and technology: Fundamentals and developments*; CRC Press: Boca Raton, Florida, USA, 2019. ISBN: 978-04-294-6534-5.
- [24] Simeonova R and Danchev N **2013** Assessment of surgical sutures POLYMED by intracutaneous irritation test in rabbits *Interdiscip. Toxicol.*, **6**, 99-102
- [25] dos Santos V, Brandalise R N and Savaris M *Engineering of biomaterials*; Springer Int. Publishing: Cham, Germany, 2017. ISBN: 978-3-319-58607-6.
- [26] Int. Standard ISO 10993-18. Biological evaluation of medical devices - Part 18: Chemical characterization of materials, July 2005.
- [27] Anderson J M, Rodriguez A and Chang D T **2008** Foreign body reaction to biomaterials. *Semin. Immunol.*, **20**, 86-100.
- [28] Hasirci V and Hasirci N *Fundamentals of biomaterials*; Springer New York: New York, USA, 2018. ISBN: 978-1-4939-8854-9.
- [29] Fraden J *Handbook of Modern Sensors*; Springer Int. Publishing: Cham, Germany, 2016. ISBN: 978-3-319-19303-8.
- [30] Carter M T, Stetter J R, Findlay M W and Patel V. **2014** Amperometric gas sensors with ionic liquid electrolytes. *ECS Trans.*, **58**, 7-18.
- [31] Schenk E H, Burke P A and Centanni M A Amperometric Gas Sensor. U.S. Patent 10,001,455, 4 October 2016.
- [32] Guth U, Gerlach F, Decker M, Oelßner W and Vonau W **2009** Solid-state reference electrodes for potentiometric sensors. *J. Solid State Electrochem.*, **13**, 27-39.
- [33] Moya A, Pol R, Martínez-Cuadrado A, Villa R, Gabriel G and Baeza M **2019** Stable full-inkjet-printed solid-state Ag/AgCl reference electrode. *Anal. Chem.*, **91**, 15539-15546.
- [34] Einaga Y, Tribidasarianggraningrum I, Ishii Y, Sekiguchi S and Murata K Ozone water concentration measurement apparatus and ozone water concentration measurement method, 2017. US Patent 9,625,405.
- [35] Ishii Y, Ivandini T A, Murata K and Einaga Y **2013** Development of electrolyte-free ozone sensors using boron-doped diamond electrodes. *Anal. Chem.*, **85**, 4284-4288.
- [36] Janknecht P, Picard C, Larbot A and Wilderer P A **2004** Membrane ozonation in wastewater treatment. *Acta Hydrochim. Hydrobiol.*, **32**, 33-39.
- [37] Kang G, Zhu Z, Tang B H, Wu C H and Wu R J **2017** Rapid detection of ozone in the parts per billion range using a novel Ni-Al layered double hydroxide. *Sens. Actuators, B*, **241**, 1203-1209.
- [38] Addanki S and Nedumaran D **2017** Fabrication of ozone sensors on porous glass substrates using gold and silver thin films nanoislands. *Optik*, **150**, 11-21.
- [39] Izumi K, Utiyama M and Maruo Y Y **2017** A porous glass-based ozone sensing chip impregnated with potassium iodide and α -cyclodextrin. *Sens. Actuators, B*, **241**, 116-122.
- [40] Wu C H, Chou T L and Wu R J **2018** Rapid detection of trace ozone in TiO_2 - In_2O_3 materials by using the differential method. *Sens. Actuators, B*, **255**, 117-124.
- [41] Jayachandiran J, Arivanandhan M, Padmaraj O, Jayavel R and Nedumaran D **2020** Investigation on ozone-sensing characteristics of surface sensitive hybrid rGO/ WO_3 nanocomposite films at ambient temperature. *Adv. Compos. Hybrid Mater.*, **3**, 16-30.
- [42] Sui Y, Liang H, Chen Q, Huo W, Du X and Mei Z **2020** Room-temperature ozone sensing capability of IGZO-decorated amorphous Ga_2O_3 films. *ACS Appl. Mater. Interfaces*, **12**, 8929-8934.
- [43] Rocha L, Foschini C R, Silva C C, Longo E and Simões A Z **2016** Novel ozone gas sensor based on ZnO nanostructures grown by the microwave-assisted hydrothermal route. *Ceram. Int.*, **42**, 4539-4545.
- [44] Moya A Integrated sensors for overcoming organ-on-a-chip monitoring challenges. Phd dissertation, Universitat Autònoma de Barcelona, 2017.
- [45] Petersen K E **1982** Silicon as a mechanical material. *Proc. of the IEEE*, **70**, 420-457.

- [46] Fang Y and Tentzeris M M Surface modification of polyimide films for inkjet-printing of flexible electronic devices. In *Flexible electronics*; Rackauskas S, Ed.; IntechOpen: London, United Kingdom, 2018. ISBN: 978-1-78923-456-5.
- [47] Kim S, Shamim A, Georgiadis A, Aubert H and Tentzeris M M **2016** Fabrication of fully inkjet-printed Vias and SIW structures on thick polymer substrates. *IEEE Trans. Compon., Packag., Manuf. Technol.*, **6**, 486–496.
- [48] Moya A, Ortega-Ribera M, Guimerà X, Sowade E, Zea M, Illa X, Ramon E, Villa R, Gracia-Sancho J and Gabriel G **2018** Online oxygen monitoring using integrated inkjet-printed sensors in a liver-on-a-chip system. *Lab Chip*, **18**, 2023–2035.
- [49] Htwe Y, Chow W S, Suriati G, Thant A A and Mariatti M **2019** Properties enhancement of graphene and chemical reduction silver NPs conductive inks printed on polyvinyl alcohol substrate. *Synth. Met.*, **256**, 116120.
- [50] Mikkonen R, Puistola P, Jönkkäri I and Mäntysalo M **2020** Inkjet printable polydimethylsiloxane for all-inkjet-printed multilayered soft electrical applications. *ACS Appl. Mater. Interfaces*, **12**, 11990–11997.
- [51] Sturgess C, Tuck C J, Ashcroft I A and Wildman R D **2017** 3D reactive inkjet printing of polydimethylsiloxane. *J. Mater. Chem. C*, **5**, 9733–9743.
- [52] Becker H and Locascio L E **2002** Polymer microfluidic devices. *Talanta*, **56**, 267–287.
- [53] Shanbhag P V and Sirkar K K **1998** Ozone and oxygen permeation behavior of silicone capillary membranes employed in membrane ozonators. *J. Appl. Polym. Sci.*, **69**, 1263–1273.
- [54] Zoumpouli G, Baker R, Taylor C, Chippendale M, Smithers C, Xian S, Mattia D, Chew Y and Wenk, J. **2018** A single tube contactor for testing membrane ozonation. *Water*, **10**, 1416.
- [55] Cui Z *Printed electronics: Materials, technologies and applications*; Higher Education Press: Hoboken, New Jersey, USA, 2016. ISBN: 9781118920923.
- [56] Tsai Y T, Chang S J, Tang I T, Hsiao Y J and Ji L W **2018** High density novel porous ZnO nanosheets based on a microheater chip for ozone sensors. *IEEE Sens. J.*, **18**, 5559–5565.
- [57] Joshi N, da Silva L F, Shimizu F M, Mastelaro V R, M'Peko J C, Lin L and Oliveira, O N **2019** UV-assisted chemiresistors made with gold-modified ZnO nanorods to detect ozone gas at room temperature. *Microchim. Acta*, **186**, 418.
- [58] Ziegler D, Bekyarova E, Marchisio A, Tulliani J M and Naishadham K Highly selective ozone sensors based on functionalized carbon nanotubes. *Proc. of the IEEE SENSORS Conf.*, New Delhi, India, 28-31 October 2018, 1-4.
- [59] Bernardini S, Benckekroum M H, Fiorido T, Aguir K, Bendahan M, Dkhil S B, Gaceur M, Ackermann J, Margeat O and Videlot-Ackermann C Ozone sensors working at room temperature using zinc oxide nanocrystals annealed at low temperature. *Proc. of the Eurosensors Conf.*, Paris, France, 3–6 September 2017, 423.
- [60] Spinelle L, Gerboles M, Aleixandre M and Bonavitacola F **2016** Evaluation of metal oxides sensors for monitoring of O₃ in ambient air at ppb level. *Chemical Engineering Transaction*, **54**, 319–324.
- [61] Korotcenkov G, Brinzari V and Cho B K **2016** In₂O₃- and SnO₂-based thin film ozone sensors: Fundamentals. *J. Sens.*, **2016**, 1–31.
- [62] Batzill M and Diebold U **2005** The surface and materials science of tin oxide. *Prog. Surf. Sci.*, **79**, 47–154.
- [63] Park Y, Dong K Y, Lee J, Choi J, Bae G N and Ju B K **2009** Development of an ozone gas sensor using single-walled carbon nanotubes. *Sens. Actuators, B*, **140**, 407–411.
- [64] Colindres S C, Aguir K, Cervantes Sodi F, Vargas L V, Salazar J M and Febles V G **2014** Ozone sensing based on palladium decorated carbon nanotubes. *Sensors*, **14**, 6806–6818.
- [65] Ghaddab B, Sanchez J B, Mavon C, Paillet M, Parret R, Zahab A A, Bantignies J L, Flaud V, Beche E and Berger F **2012** Detection of O₃ and NH₃ using hybrid tin dioxide/carbon nanotubes sensors: Influence of materials and processing on sensor's sensitivity. *Sens. Actuators, B*, **170**, 67–74.

Biocompatibility for inkjet-printed ozone sensors

31

- material for biological applications. *Structure and Applications*, 145.
- [87] Green R A, Lovell N H, Wallace G G and Poole-Warren L A **2008** Conducting polymers for neural interfaces: challenges in developing an effective long-term implant. *Biomaterials*, **29**, 3393–3399.
- [88] Scientific Polymer Products. Data sheet PSS 25704-18-1, (accessed on: 30 September 2021). Available online: <https://scipoly.com/wp-content/uploads/2020/09/Sodium%20polystyrene%20sulfonate-sds.pdf>.
- [89] INEOS. Data sheet PET 9002-88-4, (accessed on: 30 September 2021). Available online: <https://www.ineos.com/show-document/?grade=G50-100&bu=INEOS+0+%26+P+USA&documentType=SDS&docLanguage=CA-EN&version=e84c7003ec56c432cae3f968bf14c69b>.
- [90] REACH. Data sheet PMMA, (accessed on: 30 September 2021). Available online: https://www.sumitomo-chem.com.sg/wp-content/uploads/2019/09/SDS-09-0041_PMMA_PRIME_EX_EXN_MH_20190108.pdf.
- [91] Heraeus. Data sheet Platin 7440-06-4, (accessed on: 29 September 2021). Available online: https://www.heraeus.com/media/media/hpm/doc_hpm/safety_data_sheets/de_1/Platin.pdf.
- [92] DuPont. Data sheet PTFE 9002-84-0, (accessed on: 30 September 2021). Available online: <http://www1.msdirect.com/MSDS/MSDS00014/48703219-20110702.PDF>.
- [93] DeMerlis C and Schoneker D **2003** Review of the oral toxicity of polyvinyl alcohol (PVA). *Food Chem. Toxicol.*, **41**, 319–326.
- [94] A & C Plastics. Data sheet PVC 9002-86-2, (accessed on: 30 September 2021). Available online: https://www.acplasticsinc.com/media/documents/MSDS_Type1PVC.pdf.
- [95] MTI Japan. Data sheet PVDF, (accessed on: 30 September 2021). Available online: https://www.mti-japan.com/wp/wp-content/uploads/2014/08/MSDS_PVDF.pdf.
- [96] Safe Silica. Data sheet Quartz, (accessed on: 30 September 2021). Available online: <https://safesilica.eu/wp-content/uploads/2018/05/Quartz-SDS-template.pdf>.
- [97] Sciencelab. Data sheet Si 7440-21-3, (accessed on: 4 October 2021). Available online: <https://louisville.edu/micronano/files/documents/safety-data-sheets-sds/silicon/>.
- [98] Washington Mills. Data sheet SiO_2/Si 7631-86-9, (accessed on: 30 September 2021). Available online: https://www.washingtonmills.com/sites/default/files/2019-02/sds_silicon_dioxide_fused_silica_june_2018_0.pdf.
- [99] Ionic Liquids Technologies. Data sheet SnO_2 18282-10-5, (accessed on: 4 October 2021). Available online: <https://nanomaterials.iolitec.de/sites/nanomaterials.iolitec.de/files/sds/SDS%20NO-0009%20SnO2.pdf>.
- [100] Shi H, Magaye R, Castranova V and Zhao J **2013** Titanium dioxide nanoparticles: a review of current toxicological data. *Part. Fibre Toxicol.*, **10**, 1–33.
- [101] Optron. Data sheet Tungsten Trioxide 215-231-4, (accessed on: 30 September 2021). Available online: https://optron.canon/ja/support/img/pdf/en_18/optical_en/214_W03_d_en.pdf.
- [102] ECHA. Data sheet Zinc oxide 1314-13-2, (accessed on: 30 September 2021). Available online: <https://echa.europa.eu/de/registration-dossier/-/registered-dossier/16139/7/3/1>.
- [103] Saint-Gobain. Data sheet Zirconium dioxide 1314-23-4, (accessed on: 30 September 2021). Available online: <https://www.dawson-macdonald.com/wp-content/uploads/sds-alumina-zirconia.pdf>.
- [104] Andò B, Baglio S, Bulsara A R, Emery T, Marletta V and Pistorio A **2017** Low-cost inkjet printing technology for the rapid prototyping of transducers. *Sensors*, **17**, 748.
- [105] Oktavianty O, Ishii Y, Haruyama S, Kyoutani T, Darmawan Z and Swara S E **2021** Controlling droplet behaviour and quality of DoD inkjet printer by designing actuation waveform for multi-drop method. *IOP Conf. Ser.: Mater. Sci. Eng.*, **1034**, 012091.
- [106] Sekitani T, Noguchi Y, Zschieschang U, Klauk H and Someya T **2008** Organic transistors manufactured using inkjet technology with subfemtoliter accuracy. *Proceedings of the National*

Biocompatibility for inkjet-printed ozone sensors

32

- Academy of Sciences*, **105**, 4976–4980.
- [107] Kwon K-S, Rahman M K, Phung T H, Hoath S, Jeong S and Kim J S **2020** Review of digital printing technologies for electronic materials. *Flexible Printed Electron.*, **3**, 042001.
- [108] SIJ Technology. Product Line-up, (accessed on: 5 October 2021). Available online: <https://sijtechnology.com/en/products/#pro1>.
- [109] Fukuda K and Someya T **2017** Recent progress in the development of printed thin-film transistors and circuits with high-resolution printing technology. *Adv. Mater.*, **29**, 1602736.
- [110] Hassan B, Liang Y, Yong J, Yu Y, Ganesan K, Walla A, Evans R, Chana G, Nasr B and Skafidas E **2018** Facile fabrication of an electrolyte-gated In₂O₃ nanoparticle-based thin-film transistor uniting laser ablation and inkjet printing. *Flexible Printed Electron.*, **3**, 042001.
- [111] Gengenbach U, Ungerer M, Koker L, Reichert K M, Stiller P, Allgeier S, Köhler B, Zhu X, Huang C and Hagenmeyer V. **2020** Automated fabrication of hybrid printed electronic circuits. *Mechatronics*, **70**, 102403.
- [112] Wintermantel E and Ha S-W *Medizintechnik.*; Springer Berlin Heidelberg: Berlin, Heidelberg, 2009. ISBN: 978-3-540-93935-1.
- [113] Moya A, Sowade E, del Campo F J, Mitra K Y, Ramon E, Villa R, Baumann R R and Gabriel G **2016** All-inkjet-printed dissolved oxygen sensors on flexible plastic substrates. *Org. Electron.*, **39**, 168–176.
- [114] Nayak L, Mohanty S, Nayak S K and Ramadoss A **2019** A review on inkjet printing of nanoparticle inks for flexible electronics *J. Mater. Chem. C*, **7**, 8771–8795
- [115] Takada T, Suzuki K and Nakane M **1993** Highly sensitive ozone sensor. *Sens. Actuators, B*, **13**, 404–407.
- [116] Favi P M, Gao M, Johana Sepúlveda Arango L, Ospina S P, Morales M, Pavon J J and Webster T J **2015** Shape and surface effects on the cytotoxicity of nanoparticles: Gold nanospheres versus gold nanostars. *J. Biomed. Mater. Res., Part A*, **103**, 3449–3462.
- [117] Akter M, Sikder M T, Rahman M M, Ullah A K M A, Hossain K F B, Banik S, Hosokawa T, Saito T and Kurasaki M **2018** A systematic review on silver nanoparticles-induced cytotoxicity: Physicochemical properties and perspectives. *J. Adv. Res.*, **9**, 1–16.
- [118] Katsnelson B A *et al.* **2011** Subchronic systemic toxicity and bioaccumulation of Fe₃O₄ nano- and microparticles following repeated intraperitoneal administration to rats. *Int. J. Toxicol.*, **30**, 59–68.
- [119] Raju H B, Hu Y, Vedula A, Dubovy S R and Goldberg J L **2011** Evaluation of magnetic micro- and nanoparticle toxicity to ocular tissues. *PLoS One*, **6**, e17452.
- [120] Fröhlich E **2012** The role of surface charge in cellular uptake and cytotoxicity of medical nanoparticles. *Int. J. Nanomed.*, **7**, 5577–5591.
- [121] Okuda-Shimazaki J, Takaku S, Kanehira K, Sonezaki S and Taniguchi A **2010** Effects of titanium dioxide nanoparticle aggregate size on gene expression. *Int. J. Mol. Sci.*, **11**, 2383–2392.
- [122] Poland C A, Duffin R, Kinloch I, Maynard A, Wallace W A H, Seaton A, Stone V, Brown S, Macnee W and Donaldson K **2008** Carbon nanotubes introduced into the abdominal cavity of mice show asbestos-like pathogenicity in a pilot study. *Nat. Nanotechnol.*, **3**, 423–428.
- [123] Takagi A, Hirose A, Nishimura T, Fukumori N, Ogata A, Ohashi N, Kitajima S and Kanno J **2008** Induction of mesothelioma in p53+/- mouse by intraperitoneal application of multi-wall carbon nanotube. *The Journal of Toxicological Sciences*, **33**, 105–116.
- [124] Yang K and Ma Y Q **2010** Computer simulation of the translocation of nanoparticles with different shapes across a lipid bilayer. *Nat. Nanotechnol.*, **5**, 579–583.
- [125] Chu Z *et al.* **2014** Unambiguous observation of shape effects on cellular fate of nanoparticles. *Sci. Rep.*, **4**, 4495.
- [126] Nasir I, Lundqvist M and Cabaleiro-Lago C **2015** Size and surface chemistry of nanoparticles lead to a variant behavior in the unfolding dynamics of human carbonic anhydrase. *Nanoscale*, **7**, 17504–17515.
- [127] Schaeublin N M, Braydich-Stolle L K, Schrand A M, Miller J M, Hutchison J, Schlager J J

- and Hussain S M **2011** Surface charge of gold nanoparticles mediates mechanism of toxicity. *Nanoscale*, **3**, 410–420.
- [128] Goodman C M, McCusker C D, Yilmaz T and Rotello V M **2004** Toxicity of gold nanoparticles functionalized with cationic and anionic side chains. *Bioconjugate Chem.*, **15**, 897–900.
- [129] Baek M, Kim I S, Yu J, Chung H E, Choy J H and Choi S J **2011** Effect of different forms of anionic nanoclays on cytotoxicity. *J. Nanosci. Nanotechnol.*, **11**, 1803–1806.
- [130] Bhattacharjee S, de Haan L H J, Evers N M, Jiang X, Marcelis A T M, Zuilhof H, Rietjens I M C M and Alink G M **2010** Role of surface charge and oxidative stress in cytotoxicity of organic monolayer-coated silicon nanoparticles towards macrophage NR8383 cells. *Part. Fibre Toxicol.*, **7**, 25.
- [131] Cox R D and Phillips W J **2004** Ethylene glycol toxicity. *Mil. Med.*, **169**, 660–663.
- [132] Sigma-Aldrich. Safety data sheet ethyleneglycol, (accessed on: 7 August 2020). Available online: <https://www.sigmaaldrich.com/catalog/product/sial/324558?lang=de®ion=DE>.
- [133] Khan I, Saeed K and Khan I **2019** Nanoparticles: Properties, applications and toxicities. *Arabian J. Chem.*, **12**, 908–931.
- [134] Greulich C, Kittler S, Epple M, Muhr G and Köller M **2009** Studies on the biocompatibility and the interaction of silver nanoparticles with human mesenchymal stem cells (hMSCs). *Langenbeck's Archives of Surgery*, **394**, 495–502.
- [135] Tang J *et al.* **2010** Silver nanoparticles crossing through and distribution in the blood-brain barrier in vitro. *J. Nanosci. Nanotechnol.*, **10**, 6313–6317.
- [136] Lee I, Kim S, Yun J, Park I and Kim T.-S. **2012** Interfacial toughening of solution processed Ag nanoparticle thin films by organic residuals. *Nanotechnology*, **23**, 485704.
- [137] Sigma-Aldrich. Safety data sheet silver dispersion, (accessed on: 30 May 2020). Available online: <https://www.sigmaaldrich.com/catalog/product/aldrich/736465?lang=de®ion=DE>.
- [138] ANP Co. Ltd. Silver Jet Ink, (accessed on 03 August 2020). Available online: http://anapro.com/eng/product/silver_inkjet_ink.html#.
- [139] Sigma-Aldrich. Safety data sheet TGME, (accessed on: 26 July 2020). Available online: <https://www.sigmaaldrich.com/catalog/product/aldrich/568554?lang=de®ion=DE>.
- [140] Lieber C S **1988** Biochemical and molecular basis of alcohol-induced injury to liver and other tissues. *N. Engl. J. Med.*, **319**, 1639–1650.
- [141] Wang D, Ba D, Hao Z, Li Y, Sun F, Liu K, Du G and Mei Q **2018** A novel approach for PDMS thin films production towards application as substrate for flexible biosensors. *Mater. Lett.*, **221**, 228–231.
- [142] Schoen F J, Lemons J E, Ratner B D and Hoffman A S *Biomaterials science : An introduction to materials in medicine*, 3 ed., Academic Press: Burlington, USA, 2013. ISBN: 978-00-8087-780-8.
- [143] Bélanger M C and Marois Y **2001** Hemocompatibility, biocompatibility, inflammatory and in vivo studies of primary reference materials low-density polyethylene and polydimethylsiloxane: A review. *J. Biomed. Mater. Res.*, **58**, 467–477.
- [144] Lee D S, Kim S J, Sohn J H, Kim I G, Kim S W, Sohn D W, Kim J H and Choi B **2012** Biocompatibility of a PDMS-coated micro-device: Bladder volume monitoring sensor. *Chin. J. Polym. Sci.*, **30**, 242–249.
- [145] Nemani K V, Moodie K L, Brennick J B, Su A and Gimi B **2013** In vitro and in vivo evaluation of SU-8 biocompatibility. *Mater. Sci. Eng., C*, **33**, 4453–4459.
- [146] Ereifej E S, Khan S, Newaz G, Zhang J, Auner G W and VandeVord P J **2010** Characterization of astrocyte reactivity and gene expression on biomaterials for neural electrodes. *J. Biomed. Mater. Res.*, **99**, 141–150.
- [147] Kotzar G, Freas M, Abel P, Fleischman A, Roy S, Zorman C, Moran J M and Melzak J **2002** Evaluation of MEMS materials of construction for implantable medical devices. *Biomaterials*, **23**, 2737–2750.
- [148] Vernekar V N, Cullen D K, Fogleman N, Choi Y, García A J, Allen M G, Brewer G J and LaPlaca

- M C **2009** SU-8 2000 rendered cytocompatible for neuronal bioMEMS applications. *J. Biomed. Mater. Res., Part A*, **89**, 138–151.
- [149] Campbell N A, Reece J B, Urry L A, Cain M L, Wasserman S A, Minorsky P V and Jackson R B *Biology*, 8 ed., Pearson: San Francisco, USA, 2010. ISBN: 978-08-0536-844-4.
- [150] PubChem. Potassium sulfate, (accessed on: 7 August 2020). Available online: <https://pubchem.ncbi.nlm.nih.gov/compound/Potassium-sulfate#section=Absorption-Distribution-and-Excretion>.
- [151] Bedale W, Sindelar J J and Milkowski A L **2016** Dietary nitrate and nitrite: Benefits, risks, and evolving perceptions. *Meat Sci.*, **120**, 85–92.
- [152] Ma L, Hu L, Feng X and Wang S **2018** Nitrate and nitrite in health and disease. *Aging and Disease*, **9**, 938–945.
- [153] Bryan N S, Alexander D D, Coughlin J R, Milkowski A L and Boffetta P **2012** Ingested nitrate and nitrite and stomach cancer risk: An updated review. *Food Chem. Toxicol.*, **50**, 3646–3665.
- [154] Priyamvada S, Saksena S, Alrefai W A and Dudeja P K Intestinal anion absorption. In *Physiology of the Gastrointestinal Tract*, Ghishan F K and Said H M, Eds., Academic Press: London, United Kingdom, 2018, pp. 1317–1362. ISBN: 978-01-2809-954-4.
- [155] Rex D K, Di Palma J A, Rodriguez R, McGowan J and Cleveland M **2010** A randomized clinical study comparing reduced-volume oral sulfate solution with standard 4-liter sulfate-free electrolyte lavage solution as preparation for colonoscopy. *Gastrointestinal Endoscopy*, **72**, 328–336.
- [156] van Haywood B, Cordero R, Wright K, Gendreau L, Rupp R, Kotler M, Littlejohn S, Fabyanski J and Smith S **2005** Brushing with a potassium nitrate dentifrice to reduce bleaching sensitivity. *The Journal of Clinical Dentistry*, **16**, 17–22.
- [157] European Parliament and Council. Regulation (EC) No 1333/2008 of the European Parliament and of the Council of 16 December 2008 on food additives, (accessed on 31 March 2021). Available online: <https://eur-lex.europa.eu/legal-content/EN/TXT/?uri=celex%3A32008R1333>.
- [158] Brummer S B and Turner M J **1977** Electrical stimulation with Pt electrodes: II-estimation of maximum surface redox (theoretical non-gassing) limits. *IEEE Trans. Biomed. Eng.*, **24**, 440–443.
- [159] Agnew W F, Yuen T, McCreery D B and Bullara L A **1986** Histopathologic evaluation of prolonged intracortical electrical stimulation. *Exp. Neurol.*, **92**, 162–185.
- [160] Cowley A and Woodward B **2011** A healthy future: Platinum in medical applications. *Platinum Met. Rev.*, **55**, 98–107.
- [161] Özkan M, Hashmi S G, Halme J, Karakoç A, Sarikka T, Paltakari J and Lund P D **2017** Inkjet-printed platinum counter electrodes for dye-sensitized solar cells. *Org. Electron.*, **44**, 159–167.
- [162] Schubert M, Rebohle L, Wang Y, Fritsch M, Bock K, Vinnichenko M and Schumann T Evaluation of nanoparticle inks on flexible and stretchable substrates for biocompatible application. *Proc. of the 7th Electronic System-Integration Technology Conf. (ESTC)*, 18-21 September 2018, Dresden, Germany., 2018.
- [163] Int. Standard ISO 10993-5. Biological evaluation of medical devices - Part 5: Tests for in vitro cytotoxicity, June 2009.
- [164] Korotcenkov G **2007** Metal oxides for solid-state gas sensors: What determines our choice? *Mater. Sci. Eng., B*, **139**, 1–23.
- [165] Marezio M **1966** Refinement of the crystal structure of In_2O_3 at two wavelengths. *Acta Crystallogr.*, **20**, 723–728.
- [166] Garlapati S K, Mishra N, Dehm S, Hahn R, Kruk R, Hahn H and Dasgupta S **2013** Electrolyte-gated, high mobility inorganic oxide transistors from printed metal halides. *ACS Appl. Mater. Interfaces*, **5**, 11498–11502.
- [167] Dasgupta S, Kruk R, Mechau N and Hahn H **2011** Inkjet printed, high mobility inorganic-oxide field effect transistors processed at room temperature. *ACS Nano*, **5**, 9628–9638.

- [168] Bomhard E M **2018** The toxicology of indium oxide. *Environ. Toxicol. Pharmacol.*, **58**, 250–258.
- [169] Kim S H, Jeon S, Lee D K, Lee S, Jeong J, Kim J S and Cho W S **2020** The early onset and persistent worsening pulmonary alveolar proteinosis in rats by indium oxide nanoparticles. *Nanotoxicology*, **14**, 468–478.
- [170] Castronovo F P and Wagner H N **1971** Factors affecting the toxicity of the element indium. *Br. J. Exp. Pathol.*, **52**, 543–559.
- [171] Guo S, Zheng R, Jiang J, Yu J, Dai K and Yan C **2019** Enhanced thermal conductivity and retained electrical insulation of heat spreader by incorporating alumina-deposited graphene filler in nano-fibrillated cellulose. *Composites, Part B*, **178**, 107489.
- [172] Timofeeva E V, Gavrilov A N, McCloskey J M, Tolmachev Y V, Sprunt S, Lopatina L M and Selinger J V **2007** Thermal conductivity and particle agglomeration in alumina nanofluids: Experiment and theory. *Phys. Rev. E: Stat., Nonlinear, Soft Matter Phys.*, **76**, 061203.
- [173] Denes E, Barrière G, Poli E and Lévêque G **2018** Alumina biocompatibility. *J. Long-Term Eff. Med. Implants*, **28**, 9–13.
- [174] Mestres G, Espanol M, Xia W, Tenje M and Ott M **2016** Evaluation of biocompatibility and release of reactive oxygen species of aluminum oxide-coated materials. *ACS Omega*, **1**, 706–713.
- [175] Park G *et al.* **2014** Immunologic and tissue biocompatibility of flexible/stretchable electronics and optoelectronics. *Adv. Healthcare Mater.*, **3**, 515–525.
- [176] Huang E H, Gabler D M, Krecic M E, Gerber N, Ferguson R M and Orosz C G **1994** Differential effects of gallium nitrate on T lymphocyte and endothelial cell activation. *Transplantation*, **58**, 1216–1222.
- [177] Burns L A and Munson A E **1992** Gallium arsenide selectively inhibits T cell proliferation and alters expression of CD25 (IL-2R/p55). *The Journal of Pharmacology and Experimental Therapeutics*, **265**, 178–186.
- [178] de Jager T L, Cockrell A E and Du Plessis S S Ultraviolet light induced generation of reactive oxygen species. In *Ultraviolet Light in Human Health, Diseases and Environment*, Ahmad S I, Ed., Advances in Experimental Medicine and Biology, Springer: Cham, Germany, 2017, pp. 15–23. ISBN: 978-3-319-56017-5.
- [179] Rastogi R P, Richa., Kumar A, Tyagi M B and Sinha R P **2010** Molecular mechanisms of ultraviolet radiation-induced DNA damage and repair. *J. Nucleic Acids*, **2010**, 592980.
- [180] Hsiao I-L and Huang Y-J **2011** Effects of various physicochemical characteristics on the toxicities of ZnO and TiO₂ nanoparticles toward human lung epithelial cells. *Science of the Total Environment*, **409**, 1219–1228.
- [181] Ramsden J J Introduction to medical materials and devices. In *Joining and Assembly of Medical Materials and Devices*, Woodhead Publishing: Basel, Switzerland, 2013, pp. 3–27. ISBN: 978-18-4569-577-4.
- [182] Brunette D M, Tengvall P, Textor M and Thomsen P *Titanium in medicine: Material science, surface science, engineering, biological responses and medical applications*, Springer Science & Business Media: Berlin, Germany, 2012. ISBN: 978-3-642-56486-4.
- [183] Winter W WebElements periodic table electrical resistivity periodicity, (accessed on 19 August 2020). Available online: https://web.archive.org/web/20170324154411/https://www.webelements.com/periodicity/electrical_resistivity/.
- [184] Azad A M, Akbar S A, Mhaisalkar S G, Birkefeld L D and Goto K S **1992** Solid-state gas sensors: A review. *The Electrochemical Society*, **139**, 3690.
- [185] Bai J and Zhou B **2014** Titanium dioxide nanomaterials for sensor applications. *Chemical Reviews*, **114**, 10131–10176.
- [186] Logothetis E M and Kaiser W J **1983** TiO₂ film oxygen sensors made by chemical vapour deposition from organometallics. *Sens. Actuators*, **4**, 333–340.
- [187] Abbasi A and Sardroodi J J **2018** Investigation of the adsorption of ozone molecules on TiO₂/WSe₂ nanocomposites by DFT computations: Applications to gas sensor devices. *Appl. Surf. Sci.*, **436**, 27–41.

Biocompatibility for inkjet-printed ozone sensors 36

- [188] Zhang Y, Nayak T R, Hong H and Cai W **2013** Biomedical applications of zinc oxide nanomaterials. *Curr. Mol. Med.*, **13**, 1633–1645.
- [189] Bender M *et al.* **2002** Production and characterization of zinc oxide thin films for room temperature ozone sensing. *Thin Solid Films*, **418**, 45–50.
- [190] Geng Q, He Z, Chen X, Dai W and Wang X **2013** Gas sensing property of ZnO under visible light irradiation at room temperature. *Sens. Actuators, B*, **188**, 293–297.
- [191] Xu F and Ho H P **2017** Light-activated metal oxide gas sensors: A review. *Micromachines*, **8**, 333.
- [192] Sigma-Aldrich. Safety data sheet zinc oxide ink, (accessed on: 22 August 2020). Available online: <https://www.sigmaaldrich.com/catalog/product/aldrich/901091?lang=de®ion=DE>.
- [193] Jiang J, Pi J and Cai J **2018** The Advancing of Zinc Oxide Nanoparticles for Biomedical Applications. *Bioinorg. Chem. Appl.*, **2018**, 1062562.
- [194] Määttänen A, Vanamo U, Ihalainen P, Pulkkinen P, Tenhu H, Bobacka J and Peltonen J **2013** A low-cost paper-based inkjet-printed platform for electrochemical analyses. *Sens. Actuators, B*, **177**, 153–162.
- [195] Abrar M A, Dong Y, Lee P K and Kim W S **2016** Bendable electro-chemical lactate sensor printed with silver nano-particles. *Sci. Rep.*, **6**, 1–9.
- [196] Neri G, Bonavita A, Micali G, Rizzo G, Galvagno S, Niederberger M and Pinna N **2005** A highly sensitive oxygen sensor operating at room temperature based on platinum-doped In₂O₃ nanocrystals. *Chemical Communications*, **48**, 6032–6034.
- [197] Leppäniemi J, Eiroma K, Majumdar H and Alastalo A **2017** Far-UV annealed inkjet-printed In₂O₃ semiconductor layers for thin-film transistors on a flexible polyethylene naphthalate substrate. *ACS Appl. Mater. Interfaces*, **9**, 8774–8782.
- [198] Hong S, Shin J, Hong Y, Wu M, Jeong Y, Jang D, Jung G, Bae J H and Lee J H **2019** Humidity-sensitive field effect transistor with In₂O₃ nanoparticles as a sensing layer. *J. Nanosci. Nanotechnol.*, **19**, 6656–6662.
- [199] Schwartz G, Tee B C K, Mei J, Appleton A L, Kim D H, Wang H and Bao Z **2013** Flexible polymer transistors with high pressure sensitivity for application in electronic skin and health monitoring. *Nat. Commun.*, **4**, 1–8.
- [200] Chen L, An X, Jing J, Jin H, Chu Z and Li K H **2020** Ultracompact chip-scale refractometer based on an InGaN-based monolithic photonic chip. *ACS Appl. Mater. Interfaces*, **12**, 49748–49754.
- [201] Wong Y C, Ang B C, Haseeb A, Baharuddin A A and Wong Y H **2019** Conducting polymers as chemiresistive gas sensing materials: A review. *J. Electrochem. Soc.*, **167**, 037503.
- [202] Gorshelev V, Serdyuchenko A, Weber M, Chehade W and Burrows J P **2014** High spectral resolution ozone absorption cross-sections – Part 1: Measurements, data analysis and comparison with previous measurements around 293 K. *Atmos. Meas. Tech.*, **7**, 609–624.
- [203] Wu R J, Chiu Y C, Wu C H and Su Y J **2015** Application of Au/TiO₂–WO₃ material in visible light photoreductive ozone sensors. *Thin Solid Films*, **574**, 156–161.
- [204] Wei B Y, Hsu M C, Su P G, Lin H M, Wu R J and Lai H J **2004** A novel SnO₂ gas sensor doped with carbon nanotubes operating at room temperature. *Sens. Actuators, B*, **101**, 81–89.
- [205] Smith N L, Wilson A L, Gandhi J, Vatsia S and Khan S A **2017** Ozone therapy: an overview of pharmacodynamics, current research, and clinical utility. *Med. Gas Res.*, **7**, 212